



저작자표시-비영리-변경금지 2.0 대한민국

이용자는 아래의 조건을 따르는 경우에 한하여 자유롭게

- 이 저작물을 복제, 배포, 전송, 전시, 공연 및 방송할 수 있습니다.

다음과 같은 조건을 따라야 합니다:



저작자표시. 귀하는 원저작자를 표시하여야 합니다.



비영리. 귀하는 이 저작물을 영리 목적으로 이용할 수 없습니다.



변경금지. 귀하는 이 저작물을 개작, 변형 또는 가공할 수 없습니다.

- 귀하는, 이 저작물의 재이용이나 배포의 경우, 이 저작물에 적용된 이용허락조건을 명확하게 나타내어야 합니다.
- 저작권자로부터 별도의 허가를 받으면 이러한 조건들은 적용되지 않습니다.

저작권법에 따른 이용자의 권리는 위의 내용에 의하여 영향을 받지 않습니다.

이것은 [이용허락규약\(Legal Code\)](#)을 이해하기 쉽게 요약한 것입니다.

[Disclaimer](#)

Thesis for the Degree of Master of Fisheries Science

Development of Functional Materials Inspired by Marine Organisms



Suyeob Kim

Department of Fisheries Biology

The Graduate School

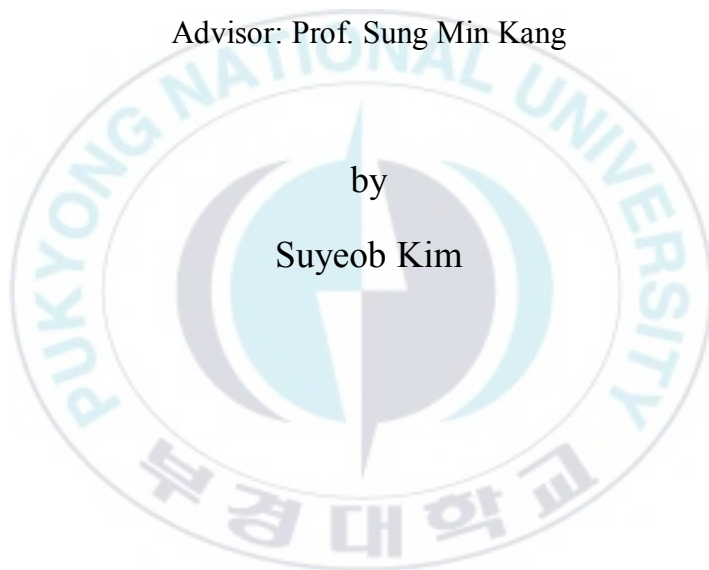
Pukyong National University

February 2016

Development of Functional Materials Inspired by Marine Organisms

해양생물을 모방한 기능성 소재 및 표면 개발 연구

Advisor: Prof. Sung Min Kang



by

Suyeob Kim

A thesis submitted in partial fulfillment of the requirements
for the degree of

Master of Fisheries Science

In the Department of Fisheries Biology, The Graduate School,
Pukyong National University

February 2016

김수엽의 수산학석사 학위논문을 인준함

2016년 2월



주심 농학박사 공승표



위원 이학박사 조우경



위원 이학박사 강성민



Development of Functional Materials Inspired by Marine Organisms

A dissertation

by

Suyeob Kim

Approved by:



(Chairman) Prof. Seung Pyo Gong



(Member) Prof. Woo Kyung Cho



(Member) Prof. Sung Min Kang

February, 2016

Contents

Contents	i
List of Figures	iii
List of Table	vi
Abstract	vii
1. Reversible Layer-by-Layer Deposition on Solid Substrates Inspired by Mussel Byssus Cuticle	1
1.1 Introduction	1
1.2 Experimental Section	3
1.2.1 Materials	3
1.2.2 Polydopamine coating	4
1.2.3 Layer-by-Layer (LbL) deposition	4
1.2.4 Characterizations	4
1.3 Results and Discussion	5
1.4 Conclusions	13
1.5 References	13
2. Versatile, Tannic Acid-Mediated Surface PEGylation for Marine Antifouling Applications	18
2.1 Introduction	18
2.2 Experimental Section	21
2.2.1 Materials	21
2.2.2 Polydopamine (pDA) coating	22
2.2.3 Tannic acid (TA) deposition	22
2.2.4 PEGylation	22
2.2.5 Protein adsorption	23
2.2.6 Diatom adhesion	23

2.2.7 Characterization	23
2.3 Results and Discussion	24
2.4 Conclusions	40
2.5 References	41
3. Construction of Anti-Bacterial Alginate Films using Catechol-Fe(III) Interactions	48
3.1 Introduction	48
3.2 Experimental Section	50
3.2.1 Materials	50
3.2.2 Synthesis of catechol-conjugated alginates (Alg-C)	51
3.2.3 Polydopamine (pDA) coating	52
3.2.4 Spin-coating of Alg-C	52
3.2.5 Stability test	53
3.2.6 Protein adsorption test	53
3.2.7 Antibacterial test	53
3.2.8 Characterizations	54
3.3 Results and Discussion	55
3.4 Conclusions	71
3.5 References	71
Abstract (Korean)	78

List of Figures

Figure 1.1 (a) A marine mussel attached to the solid substrate via byssus. (b) Schematic representation of the catechol-Fe ^{III} interactions in the byssus cuticle. (c) Schematic description of the byssus-cuticle-inspired, reversible surface chemistry.	9
Figure 1.2 (a) Chemical structure of TA, a catecholic compound. (b) Thickness of layers deposited on the Si surface after (Fe/TA) _n treatments. (c) XPS spectra of the polydopamine-coated Si surface before (left) and after (Fe/TA) ₁₀ treatments.	10
Figure 1.3 Versatility of the byssus-cuticle-inspired surface chemistry. (a) Images of unmodified (left), polydopamine-coated (middle), and (Fe/TA) ₁₀ -treated (right) Teflon surfaces. (b) Water contact angle images of unmodified (left), polydopamine-coated (middle), and (Fe/TA) ₁₀ -treated (right) Teflon surfaces. (c) XPS spectra of Teflon surfaces before and after surface treatments.	11
Figure 1.4 Reversibility of the byssus-cuticle-inspired surface chemistry. (a) Changes in the thickness of layers deposited on the catechol-functionalized Si surface after (Fe/TA) ₁₀ and EDTA treatments. (b) XPS spectrum of the (Fe/TA) ₁₀ -treated Si surface after the EDTA treatment.	12
Figure 2.1 Schematic illustration of the preparation of the marine antifouling surface coating.	31
Figure 2.2 X-ray photoelectron spectra of (a) pDA-coated, (b) pDA/TA-coated, and (c) pDA/TA/PEG-coated Si surfaces.	32
Figure 2.3 High-resolution XPS spectra (C 1s) of (a) pDA-, (b) pDA/TA-coated, and (c) pDA/TA/PEG-coated Si surfaces.	34
Figure 2.4 FT-IR spectra of (a) pDA-coated, (b) pDA/TA-coated, and (c) pDA/TA/PEG-coated Au surfaces.	35

Figure 2.5 Protein adsorption on the different coatings (substrate: Si). Each point is the mean from 15 measurements on 3 replicate samples. The error bars display the 95% confidence limits. 36

Figure 2.6 Diatom adhesion on the different coatings (substrate, stainless steel; unit area, 0.11 mm²). Each point is the mean from 60 counts on 3 replicate samples. The error bars display the 95 % confidence limits. 37

Figure 2.7 Water contact angle images of (a) non-treated, (b) pDA-, and (c) pDA/TA-coated stainless steel surfaces. 37

Figure 2.8 Stability of the pDA/TA/PEG coating in seawater (substrate: stainless steel, unit area: 0.11 mm²). Each point is the mean from 60 counts on 3 replicate samples. The error bars display the 95% confidence limits. 38

Figure 2.9 Diatom adhesion on non-treated and pDA/TA/PEG-coated nylon surfaces (unit area: 0.11 mm²). Each point is the mean from 60 counts on 3 replicate samples. The error bars display the 95% confidence limits. 39

Figure 3.1 (a) A schematic illustration of the synthesis of alginate-catechol. (b) UV-vis spectra of alginate-catechol (1 mg/mL, solid) and alginate (1 mg/mL, dash). 62

Figure 3.2 Schematic illustration of the preparation of the anti-bacterial surface coating. 63

Figure 3.3 X-ray photoelectron spectra of different coatings. 64

Figure 3.4 Thickness of Alg-C layer of the various concentration of Alg-C coating on a solid substrates. Each point is the mean from 15 measurements on 3 replicate samples. The error bars display the 95% confidence limits. 65

Figure 3.5 Thickness of Alg-C/Fe^{III}, Alg-C, Alg/Fe^{III}, and Alg layers on pDA-coated surfaces before (black) and after (yellow) chemical treatment. Each point is the mean from 15

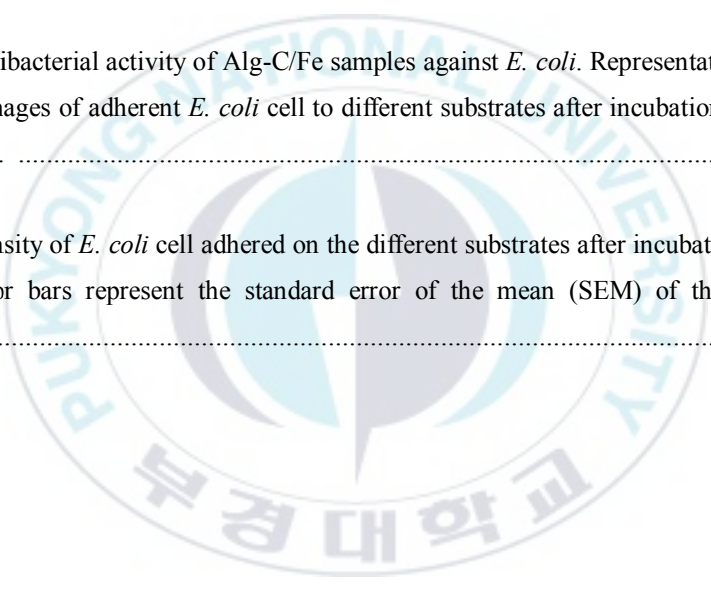
measurements on 3 replicate samples. The error bars display the 95% confidence limits. 66

Figure 3.6 (a) Thickness of Alg-C layer on surfaces before (left) and after (right) EDTA treatment. Each point is the mean from 15 measurements on 3 replicate samples. The error bars display the 95% confidence limits. (b) XPS spectrum of the Alg-C layers on surfaces before (i) and after (ii) the EDTA treatment. 67

Figure 3.7 Protein adsorption on the various thickness of Alg-C layers. Each point is the mean from 15 measurements on 3 replicate samples. The error bars display the 95% confidence limits. 68

Figure 3.8 Antibacterial activity of Alg-C/Fe samples against *E. coli*. Representative fluorescence microscopic images of adherent *E. coli* cell to different substrates after incubation for 6 h (upper) or 24 h (lower). 69

Figure 3.9 Density of *E. coli* cell adhered on the different substrates after incubation for (a) 6 h or (b) 24 h. Error bars represent the standard error of the mean (SEM) of three independent experiments. 70



List of Tables

Table 2.1 Atomic composition (%) of pDA-, pDA/TA-, and pDA/TA/PEG-coated Si surfaces.
..... 33



Development of Functional Materials Inspired by Marine Organisms

Suyeob Kim

Department of Fisheries Biology, The Graduate School,
Pukyong National University

Abstract

In recent years, non-biofouling surface has been interested for applications in medical devices, biosensor, and marine equipments. Various materials including polysaccharides, polyethylene glycol (PEG), and zwitterionic polymers have been investigated to generate non-biofouling surfaces. Although the above-mentioned materials have been successfully implemented for non-biofouling surface preparation, complicated chemical reactions and material dependent properties were considered to be significant drawbacks. To solve the problem, we developed a facile and material-independent surface coating method using a mussel-inspired functional material, polydopamine. Combination of mussel-inspired polydopamine and non-biofouling materials enabled the introduction of non-biofouling property onto the various surfaces. In chapter 1, we reported that emulating the properties of the mussel byssus cuticle provides an important platform for developing reversible layer-by-layer (LbL) deposition, an advanced technique for surface modification. LbL films were constructed on solid substrates by sequential immersion of substrates into solutions containing iron (III) and catecholic compounds. In chapter 2, we reported a facile and versatile approach to the formation of marine antifouling surface coatings. The approach consists of a combined coating of polydopamine and tannic acid and subsequent immobilization of PEG on solid substrates. TA coating of a polydopamine-coated surface was carried out using iron (III) coordination chemistry, and PEG was immobilized on the TA-coated surface via hydrogen bond formation. Stainless steel and nylon were successfully modified by this approach, and the resulting substrates were used for marine antifouling applications, in which diatom adhesion was significantly inhibited. In the last chapter, we synthesized a catechol-conjugated alginate (Alg-C) to construct anti-bacterial nanofilms. The Alg-C nanofilm was formed on the polydopamine-coated surface via iron (III) coordination reaction, and the resulting surface showed excellent resistance against *E. coli* adhesion, implying the anti-bacterial property of the surface.

Chapter 1. Reversible Layer-by-Layer Deposition on Solid Substrates Inspired by Mussel Byssus Cuticle

1.1 Introduction

Control of the attachment and detachment of chemical ligands on target surfaces is an ultimate goal in surface engineering. Two conditions are needed to achieve this goal: 1) a surface coating technique that can be applied to any target substrate and 2) a route that can be combined with the surface coating method to affect reversible attachment and detachment of ligands. The first goal has been realized by mimicking mussel foot proteins (mfps), specifically, mfp-3 and -5 (Waite et al., 2001; Silverman et al., 2007). These two proteins, which contain the noncanonical amino acid 3,4-dihydroxy-L-phenylalanine (DOPA), have been found to play an important role in the underwater adhesion of mussels by inducing adhesion (Lee et al., 2011; Lee et al., 2006; 2007). After this discovery, studies have found catecholamines with structures that are highly similar to that of DOPA, and have revealed their applicability as surface-modification agents (Lee et al., 2007; Kang et al., 2009; Ye et al., 2011). Similarly, dopamine and norepinephrine have been utilized as material-independent surface coatings.

As part of investigations on material-independent surface coatings, a method

was sought to affect reversible attachment of ligands on the catecholamine-functionalized surface. Important chemical insight into this process was drawn from the extensible protective coatings of *Mytilus galloprovincialis* byssus. Mussel byssus is covered by a cuticle, which is a micrometer-thick layer. The cuticle is known to insulate the collagen core from external factors through its high hardness and extensibility (Holten-Andersen et al., 2007; 2009). According to previous reports, the cuticle is composed of metal ions and mfp-1, the latter of which consists of 15 mol% DOPA (Zhao and Waite, 2005; Sun and Waite, 2005). Complexation between DOPA and Fe^{III} gives rise to the characteristic property of mussel byssus cuticle (Figure 1.1 a and b) (Harrington et al., 2010; Wilker, 2010). Specifically, Fe^{III} can interact with up to three DOPA catechol functionalities, thereby bridging DOPA-containing proteins (Zeng et al., 2010). The catechol-Fe^{III}-catechol bridge formed in the cuticle is strong and reversible. When a large stress is applied to the byssus, the catechol-Fe^{III} interactions are cleaved; this cleavage prevents severe damage to the matrix of the byssus cuticle. Upon removal of the stress, the catechol-Fe^{III} bonding is restored. Thus, the reversible cleavage and formation of catechol-Fe^{III} interactions serve as an important tool for the survival of mussels under heavy stress caused by waves (Holten-Andersen et al., 2007). The reversibility of these interactions has been proven by studies using a surface force apparatus. Zeng et al. showed that a strong and reversible interaction forms between mfp-1 films in the presence of Fe^{III}, whereas no

interaction occurs without Fe^{III}. The interaction is drastically weakened by the addition of ethylenediaminetetraacetic acid (EDTA), a chelating agent of transition metals, and excess Fe^{III}; these observations support the existence of Fe^{III}-mediated interactions. Given the controllability of the catechol-Fe^{III} interaction, we speculated that such interactions could be used to develop reversible surface chemical interactions. Moreover, the interaction can be combined with a material-independent coating (i.e., polydopamine coating), on the surface of which catechol groups are introduced (Lee et al., 2007). Such polydopamine coating, which is thus capable of participating in catechol-Fe^{III} interactions, enables the controlled attachment or detachment of chemical ligands to its surface.

1.2 Experimental Section

1.2.1 Materials

Dopamine hydrochloride (98%, Aldrich), trizma base (99%, Sigma), trizma·HCl (99%, Sigma), ethylenediaminetetraacetic acid (EDTA, 98.5%, Sigma-Aldrich), iron(III) chloride hexahydrate (FeCl₃·6H₂O, 97%, Sigma-Aldrich), tannic acid (TA, Sigma-Aldrich), absolute ethanol (Merck), and acetone (99%, Daejung Chemicals & Metals) were used as received.

1.2.2 Polydopamine coating

Solid substrates were cleaned in acetone or ethanol with sonication prior to use. Polydopamine coating was performed by immersing substrates in a buffer solution (2 mg of dopamine hydrochloride per milliliter of 10 mM Tris, pH 8.5) at room temperature. The coated substrates were rinsed with deionized water and dried under a stream of nitrogen gas.

1.2.3 Layer-by-layer (LbL) Depositions

Polydopamine-coated substrates were transferred to ethanolic FeCl₃ (10 mM) and TA solutions (10 mM) for constructing LbL films. The following cycle was generally used: (1) FeCl₃ for 1 s, (2) rinsing with ethanol, (3) TA for 1 s, and (4) rinsing with ethanol. A control experiment was performed without FeCl₃. To test the reversibility of LbL depositions, LbL films deposited on solid substrates were removed by treatment with a solution of EDTA (1 mM, pH 3.5) for 30 min, and reconstructed by an additional LbL deposition process.

1.2.4 Characterizations

XPS spectra were obtained using a MultiLab 2000 system (Thermo VG Scientific, UK) with a Mg K α X-ray source and ultrahigh vacuum ($\sim 10^{-10}$ mbar). The thickness of organic layers on solid substrates was measured using a M-2000D ellipsometer (J. A. Woollam Co., USA). Static water contact angle

measurements were performed using a Phoenix-300 TOUCH goniometer (Surface Electro Optics Co., Ltd., Korea).

1.3 Results and Discussion

The aforementioned byssus-cuticle-inspired, reversible surface chemistry was demonstrated through a three-step procedure (Figure 1.1 c): a) introduction of catechol functionalities on the solid substrates by applying a polydopamine coating, b) immobilization of Fe^{III} on the surface catechol groups, and c) formation of catechol-Fe^{III}-catechol bridges by addition of catecholic compounds. Repetitive attachment of catecholic compounds to the surface could be carried out with unreacted catechol groups of compounds attached to the surface. Dissociation of the catechol-Fe^{III} interactions was achieved by simple immersion of substrates in a solution of EDTA. Tannic acid (TA) was chosen as a model catecholic compound because it contains various catechol functionalities and has been frequently utilized for constructing nanofilms on solid substrates (Figure 1.2 a) (Ejima et al., 2013; Shutava et al., 2005; Kozlovskaya et al., 2010). Prior to deposition of Fe^{III} and TA on the surface, a silicon (Si) substrate was pre-incubated in an alkaline dopamine solution to introduce catechol groups on its surface. Fe/TA deposition was subsequently carried out on the 8 nm thick

polydopamine-coated Si surface. A gradual increase in thickness of the deposited layers was observed as the number of Fe/TA treatments increased: the thickness was found to be 27 nm after 10 repetitive treatments of Fe/TA (denoted as (Fe/TA)₁₀) (Figure 1.2 b). Control experiments, which were carried out in the absence of Fe^{III}, did not result in an increase in thickness. Taken together, it was concluded that the LbL films were fabricated by specific interactions between catechol and Fe^{III}. Further characterization of the surface was performed by X-ray photoelectron spectroscopy (XPS). The nitrogen (N 1s) and silicon (Si 2s and 2p) peaks in the XPS spectrum of the polydopamine-coated Si surface correspond to polydopamine and the substrate, respectively (Figure 1.2 c, left). After treatment with (Fe/TA)₁₀, characteristic peaks (N 1s, Si 2s, and 2p) in the spectrum of the polydopamine-coated surface disappeared, and new peaks for iron (Fe 2p) emerged (Figure 1.2 c, right). Quantitative analysis of the surface chemical composition also supported the successful deposition of Fe/TA layers. The amounts of Fe 2p and oxygen (O 1s) increased from 0 to 3.8% and from 21.4 to 36.7%, respectively, with a concurrent decrease in the amounts of N (N 1s) and Si (Si 2s) from 8.98 to 3.3% and from 19.5 to 0%, respectively. In addition to the controlled deposition of nanometer-thick organic layers on the surface, the surface chemistry is innovative from an engineering point of view. In particular, the catechol-Fe^{III} interaction forms very rapidly; when bulk solutions of TA and Fe^{III} are mixed together, an immediate color change of the resulting solution is

observed (pale yellow→purple). This change indicates that a single layer of catecholic compounds can be deposited within a very short period of time through catechol-Fe^{III} interactions. Thus, depositions of Fe^{III} and TA layers were accomplished by sequential immersions of polydopamine-coated substrates into Fe^{III} and TA solutions.

The versatility of the byssus-cuticle-inspired surface chemistry was tested by using a Teflon surface, which is difficult to functionalize (Lee et al., 2008). Polydopamine coating and (Fe/TA)₁₀ treatment resulted in a visible change in color from white to pale brown and dark purple (Figure 1.3 a). Polydopamine, bis(catecholato)-Fe^{III}, and tris(catecholato)-Fe^{III} are known to present brown, blue, and dark red colors (Holten-Andersen et al., 2011; Xu et al., 2012), respectively; thus, these color changes imply that bis- and tris(catecholato)-Fe^{III} co-contributed to the LbL depositions on the polydopamine-coated Teflon surface. The modified surface was further characterized by water contact angle goniometry and XPS. The water contact angle sequentially decreased from 100.3° to 63.1° and then to 51.6° upon polydopamine coating and (Fe/TA)₁₀ treatment because of the hydrophilic nature of polydopamine and TA (Figure 1.3 b). XPS spectra also show that Fe/TA layers, which contain oxygen and Fe^{III}, were deposited on the Teflon surface; peaks of O 1s and Fe 2p appeared, and the intensity of the substrate peak (F 1s) significantly decreased after the surface treatment (Figure 1.3 c).

The byssus-cuticle-inspired surface chemistry is advantageous for the reversible attachment and detachment of catecholic compounds to the surface. The formed catechol-Fe^{III} interactions may be disrupted by the addition of an Fe^{III}-chelating agent, EDTA (Zeng et al., 2010; Holten-Andersen et al., 2011). After treatment with EDTA solution (1 mM, pH 3.5) for 1 h, the deposited Fe/TA layers were completely removed from the surface (Figure 1.4 a). Additionally, the XPS spectrum shows no Fe^{III} peaks generated on the surface, thereby indicating that Fe^{III} was removed from the surface through chelation with EDTA (Figure 1.4 b) (Zeng et al., 2010). The resulting surface was again used for the deposition of Fe/TA layers because the surface-bound catechol functionalities that form the catechol-Fe^{III} complex were still active. Consistent with this assumption, Fe/TA layers were reconstructed by (Fe/TA)₁₀ treatment, and the 35 nm thickness of the coating was recovered. Such reversible depositions of Fe/TA layers were repeated several times; all experiments showed nearly the same increase and decrease in thickness, thus implying the excellent reversibility of the surface chemical reaction (Figure 1.4 a).

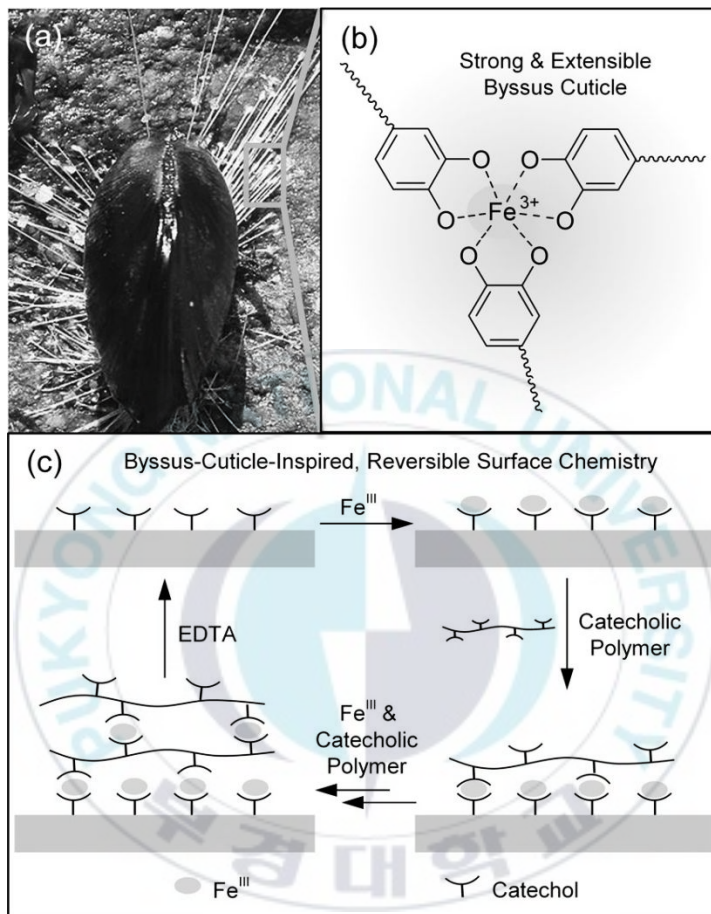


Figure 1.1 (a) A marine mussel attached to the solid substrate via byssus. (b) Schematic representation of the catechol- Fe^{III} interactions in the byssus cuticle. (c) Schematic description of the byssus-cuticle-inspired, reversible surface chemistry.

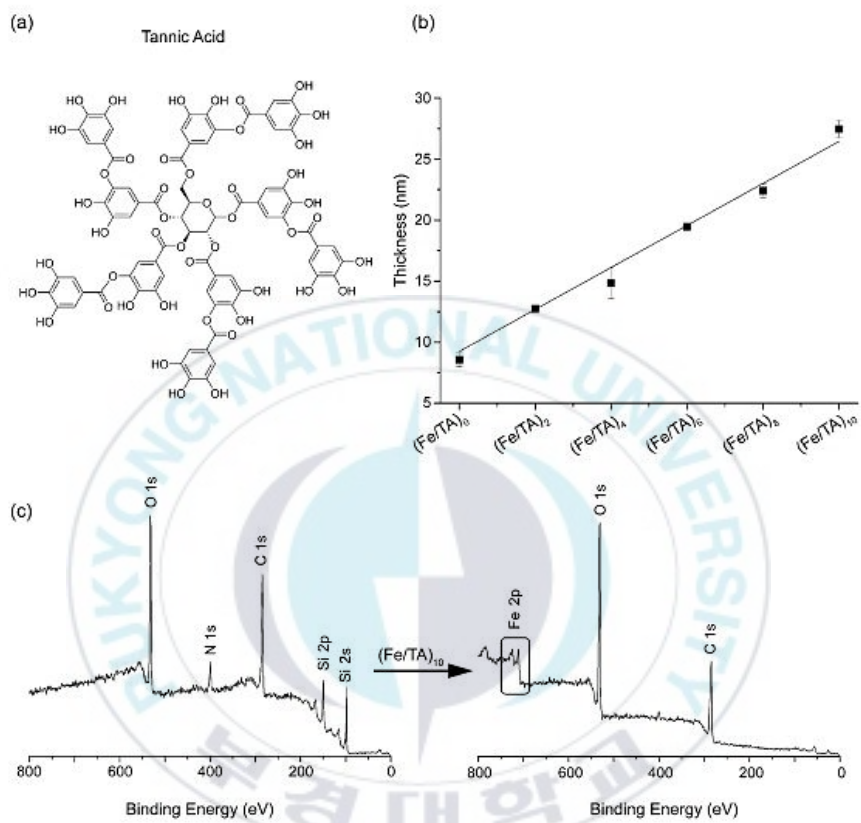


Figure 1.2 (a) Chemical structure of TA, a catecholic compound. (b) Thickness of layers deposited on the Si surface after $(\text{Fe}/\text{TA})_n$ treatments. (c) XPS spectra of the polydopamine-coated Si surface before (left) and after $(\text{Fe}/\text{TA})_{10}$ treatments.

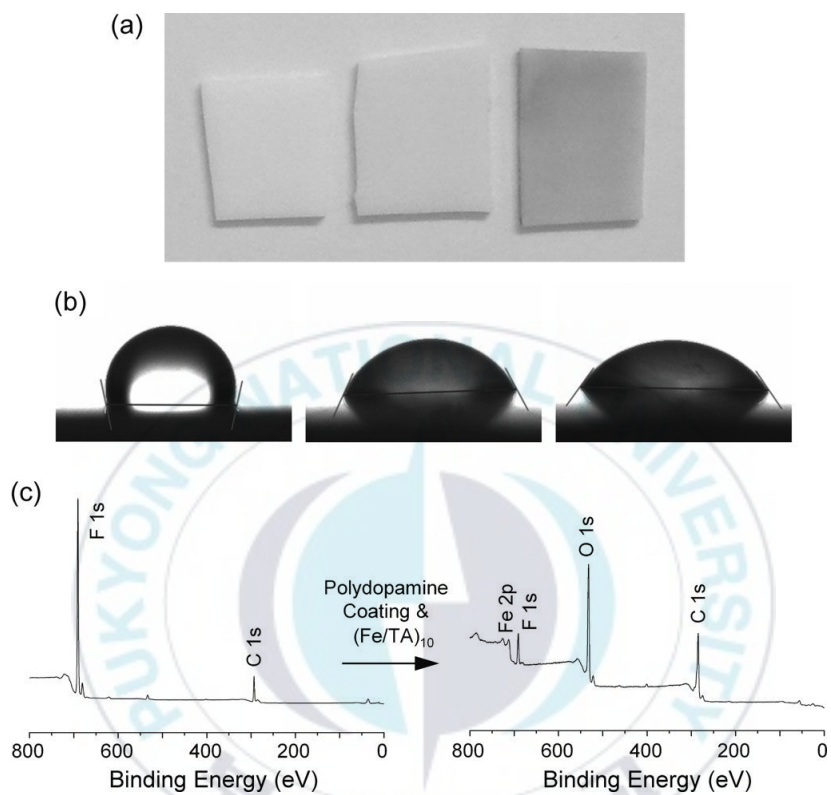


Figure 1.3 Versatility of the byssus-cuticle-inspired surface chemistry. (a) Images of unmodified (left), polydopamine-coated (middle), and $(\text{Fe}/\text{TA})_{10}$ -treated (right) Teflon surfaces. (b) Water contact angle images of unmodified (left), polydopamine-coated (middle), and $(\text{Fe}/\text{TA})_{10}$ -treated (right) Teflon surfaces. (c) XPS spectra of Teflon surfaces before and after surface treatments.

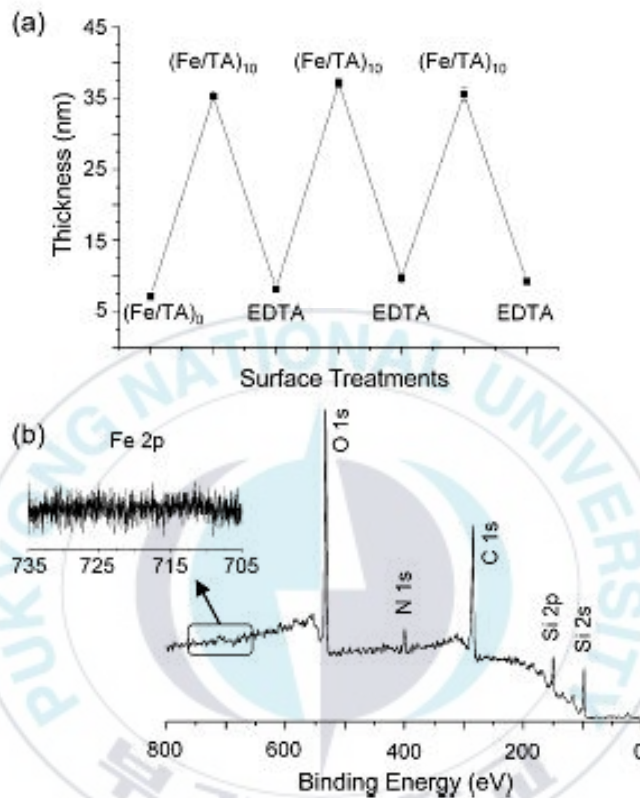


Figure 1.4 Reversibility of the byssus-cuticle-inspired surface chemistry. (a) Changes in the thickness of layers deposited on the catechol-functionalized Si surface after $(\text{Fe}/\text{TA})_{10}$ and EDTA treatments. (b) XPS spectrum of the $(\text{Fe}/\text{TA})_{10}$ -treated Si surface after the EDTA treatment.

1.4 Conclusions

In summary, we have presented a method for reversible layer-by-layer (LbL) deposition on solid substrates by mimicking the mussel byssus cuticle. Catecholic compounds and Fe^{III} that reversibly form the complex were used to construct the LbL films, and controlled deposition was achieved by sequential immersion of the substrates into a solution of each starting material. Moreover, reversible construction and deconstruction of LbL films was demonstrated by EDTA treatment of the coated substrate. We believe that the mussel-byssus-cuticle-inspired surface chemistry provides an important platform to precisely control the attachment and detachment of ligands to surfaces.

1.5 References

Ejima, H.; Richardson, J. J.; Liang, K.; Best, J. P.; van Koeveden, M. P.; Such, G. K.; Cui, J.; Caruso, F. **2013**. One-Step Assembly of Coordination Complexes for Versatile Film and Particle Engineering. *Science* *341*: 154-157.

Harrington, M. J.; Masic, A.; Holten-Andersen, N.; Waite, J. H.; Fratzl, P. **2010**. Iron-Clad Fibers: A Metal-Based Biological Strategy for Hard Flexible Coatings.

Science 328: 216-220.

Holten-Andersen, N.; Fantner, G. E.; Hohlbauch, S.; Waite, J. H.; Zok, F. W. **2007**. Protective Coatings on Extensible Biofibres. *Nat. Mater.* 6: 669-672.

Holten-Andersen, N.; Harrington, M. J.; Birkedal, H.; Lee, B. P.; Messersmith, P. B.; Lee, K. Y. C.; Waite, J. H. **2011**. pH-Induced Metal-Ligand Cross-Links Inspired by Mussel Yield Self-Healing Polymer Networks with Near-Covalent Elastic Moduli. *Proc. Natl. Acad. Sci. USA* 108: 2651-2655.

Holten-Andersen, N.; Mates, T. E.; Toprak, M. S.; Stucky, G. D.; Zok, F. W.; Waite, J. H. **2009**. Metals and the Integrity of a Biological Coating: The Cuticle of Mussel Byssus. *Langmuir* 25: 3323-3326.

Holten-Andersen, N.; Zhao, H.; Waite, J. H. **2009**. Stiff Coatings on Compliant Biofibers: The Cuticle of *Mytilus Californianus* Byssal Threads. *Biochemistry* 48: 2752-2759.

Kang, S. M.; Rho, J.; Choi, I. S.; Messersmith, P. B.; Lee, H. **2009**. Norepinephrine: Material-Independent, Multifunctional Surface Modification Reagent. *J. Am. Chem. Soc.* 131: 13224-13225.

Kozlovskaya, V.; Kharlampieva, E.; Drachuk, I.; Cheng, D.; Tsukruk, V. V. **2010**. Responsive Microcapsule Reactors Based on Hydrogen-bonded Tannic Acid Layer-by-Layer Assemblies. *Soft Matter* **6**: 3596-3608.

Lee, B. P.; Messersmith, P. B.; Israelachvili, J. N.; Waite, J. H. **2011**. Mussel-Inspired Adhesives and Coatings. *Annu. Rev. Mater. Res.* **41**: 99-132.

Lee, H.; Dellatore, S. M.; Miller, W. M.; Messersmith, P. B. **2007**. Mussel-Inspired Surface Chemistry for Multifunctional Coatings. *Science* **318**: 426-430.

Lee, H.; Lee, B. P.; Messersmith, P. B. **2007**. A Reversible Wet/Dry Adhesive Inspired by Mussels and Geckos. *Nature* **448**: 338-341.

Lee, H.; Lee, Y.; Statz, A. R.; Rho, J.; Park, T. G.; Messersmith, P. B. **2008**. Substrate-Independent Layer-by-Layer Assembly by Using Mussel-Adhesive-Inspired Polymers. *Adv. Mater.* **20**: 1619-1623.

Lee, H.; Scherer, N. F.; Messersmith, P. B. **2006**. Single-Molecule Mechanics of Mussel Adhesion. *Proc. Natl. Acad. Sci. USA* **103**: 12999-13003.

Shutava, T.; Prouty, M.; Kommireddy, D.; Lvov, Y. **2005**. pH Responsive

Decomposable Layer-by-Layer Nanofilms and Capsules on the Basis of Tannic Acid. *Macromolecules* 38: 2850-2858.

Silverman, H. G.; Roberto, F. F. **2007**. Understanding Marine Mussel Adhesion. *Mar. Biotechnol.* 9: 661-681.

Sun, C.; Waite, J. H. **2005**. Mapping Chemical Gradients within and along a Fibrous Structural Tissue, Mussel Byssal Threads. *J. Biol. Chem.* 280: 39332-39336.

Waite, J. H.; Qin, X. **2001**. Polyphosphoprotein from the Adhesive Pads of *Mytilus edulis*. *Biochemistry* 40: 2887-2893.

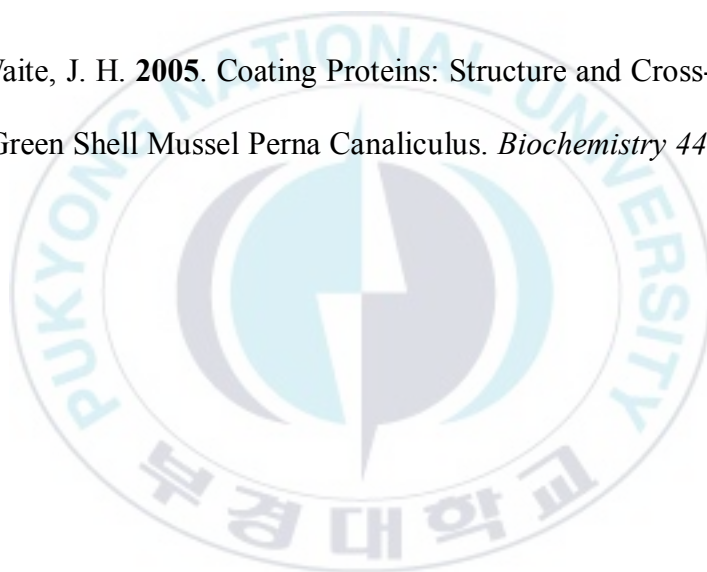
Wilker, J. J. **2010**. Das Eisenverstärkte Haftsystm von Meeresmuscheln. *Angew. Chem.* 122: 8252-8254; **2010**. The Iron-Fortified Adhesive System of Marine Mussels. *Angew. Chem. Int. Ed.* 49: 8076-8078.

Xu, H.; Nishida, J.; Ma, W.; Wu, H.; Kobayashi, M.; Otsuka, H.; Takahara, A. **2012**. Competition between Oxidation and Coordination in Cross-Linking of Polystyrene Copolymer Containing Catechol Groups. *ACS Macro Lett.* 1: 457-460.

Ye, Q.; Zhou, F.; Liu, W. **2011**. Bioinspired Catecholic Chemistry for Surface Modification. *Chem. Soc. Rev.* *40*: 4244-4258.

Zeng, H.; Hwang, D. S.; Israelachvili, J. N.; Waite, J. H. **2010**. Strong Reversible Fe³⁺-Mediated Bridging between Dopa-Containing Protein Films in Water. *Proc. Natl. Acad. Sci. USA* *107*: 12850-12853.

Zhao, H.; Waite, J. H. **2005**. Coating Proteins: Structure and Cross-Linking in fp-1 from the Green Shell Mussel *Perna Canaliculus*. *Biochemistry* *44*: 15915-15923.



Chapter 2. Versatile, Tannic Acid-Mediated Surface PEGylation for Marine Antifouling Applications

2.1 Introduction

The development of marine antifouling coatings is of importance because severe adhesion of marine organisms onto synthetic surfaces causes increased fuel consumption in marine vessels and malfunctioning of aquaculture instruments (Callow et al., 2011). To inhibit the adhesion of marine organisms onto solid substrates, paints containing biocides have generally been used, and as a result, marine fouling was effectively reduced (Lejars et al., 2012). However, an environmental issue emerged when the adverse effect of biocides was revealed (Yebra et al., 2004), and the development of environmentally friendly marine antifouling coatings is needed.

Much effort has been made to find new methods for marine antifouling coatings, with a focus on changing the surface chemical composition of solid substrates (Weinman et al., 2009; Park et al., 2010; Cho et al., 2011; Ekblad et al., 2008; Schilp et al., 2007; Statz et al., 2006; Zhang et al., 2009; Zhu et al., 2013) because the adhesion of marine organisms is known to be highly related to the surface properties of a substrate (Finlay et al., 2002; Bowen et al., 2007;

Umemura et al., 2007; Holland et al., 2004). In particular, considering that some marine organisms adhere to solid substrates using protein-containing glues (Callow et al., 2006; Wetherbee et al., 1998; Pettitt et al., 2004), protein-adsorption-resistant materials have been employed to prevent adhesion of marine organisms. For example, Schilp et al. formed hexa(ethylene glycol) (EG₆)-containing self-assembled monolayers (SAMs) on gold, and showed that OH-terminated EG₆-SAMs are highly resistant to diatom adhesion. In addition to oligo(ethylene glycol) compounds, the marine antifouling properties of poly(ethylene glycol) (PEG) were also investigated by Statz et al., who synthesized L-3,4-dihydroxyphenylalanine (DOPA)-conjugated PEG, and applied this polymer as a coating on titanium surfaces. The adhesion behavior of diatoms and *Ulva* spores on the PEG-coated surface was analyzed, and excellent antifouling and fouling release properties were identified.

Similar to the PEG coatings, superhydrophilic polymer coatings have also revealed marine antifouling abilities, as well as inhibition of protein adsorption. For instance, Zheng et al. fabricated a sulfobetaine methacrylate (SBMA)-grafted glass surface via surface-initiated atom transfer radical polymerization, and showed that diatoms are unable to adhere to the SBMA-grafted surface. Recently, superhydrophilic polymer coatings were further advanced by combining these coatings with control of the surface topography (Wan et al., 2012; 2013). Wan et al. grafted 3-sulfopropyl methacrylate (SPMA) on the surface of leaf-like

microstructures and natural fur, and found that these surfaces inhibit the adhesion of marine microorganisms very effectively. Although PEG- or superhydrophilic polymer-coated surfaces have been successfully implemented in marine antifouling applications, all examples have the critical drawback that they can only be applied to limited types of materials (Schilp et al., 2007; Statz et al., 2006; Zhang et al., 2009; Wan et al., 2012; 2013), i.e., they exhibit a lack of versatility, and advancement in coating methods is required.

Very recently, polyphenol-based surface coatings were developed (Ejima et al., 2013; Sileika et al., 2013; Kim et al., 2014; Rahim et al., 2014). Ejima et al. reported the surface coating ability of the mixture of tannic acid (TA) and Fe^{III} for the first time, and Sileika et al. reported that a TA coating can be achieved under high salt conditions (~ 0.6 M), even in the absence of Fe^{III}. Owing to the ease of use and environmental friendliness of the TA coating developed by Sileika et al., various applications were investigated, such as control of bacterial and mammalian cell adhesion, and radical scavenging. In spite of the promising applicability, there are still some limitations to TA coatings prepared under high salt conditions. The coating does not show versatility, and specific PEG compounds (thiol- or amine-conjugated PEG) are required to control cell adhesion. Meanwhile, our group reported a TA coating that consists of a material-independent polydopamine (pDA) coating and Fe^{III}-mediated TA deposition

(pDA/TA coating) (Kim et al., 2014). Given the versatility of our coating method, we speculated that combining the pDA/TA coating with the antifouling properties of PEG would yield versatile marine antifouling coatings. In fact, TA is known to be a good PEG-binding agent in food science (Jones et al., 1965; Schofield et al., 2001). Herein, we report that the pDA/TA coating can serve as an effective platform for marine antifouling surface coating preparation. Utilizing the high binding capability of TA for PEG (via hydrogen bonding), thiol- and amine-free PEG was easily immobilized on the pDA/TA-coated surface. Furthermore, the versatility of the coating enabled diverse marine antifouling coatings to be prepared.

2.2 Experimental Section

2.2.1 Materials

Dopamine hydrochloride (98%, Aldrich), Trizma base (99%, Sigma), Trizma HCl (99%, Sigma), iron(III) chloride hexahydrate ($\text{FeCl}_3 \cdot 6\text{H}_2\text{O}$, 97%, Sigma-Aldrich), tannic acid (TA, Sigma-Aldrich), fibrinogen (from human plasma, Sigma), four-arm polyethylene glycol methoxy (2k MW, SunBio), stainless steel ($\text{Fe/Cr}_{18}/\text{Ni}_{10}/\text{Mo}_3$: thickness, 0.25 mm; disc diam., 10 mm, Goodfellow), nylon (thickness, 0.5 mm; size, 50×50 mm, Goodfellow), hydrochloric acid (HCl,

Junsei), absolute ethanol (Merck), and acetone (99%, Daejung Chemicals & Metals) were used as received.

2.2.2 Polydopamine (pDA) coating

Solid substrates were cleaned in acetone or ethanol with sonication prior to use. pDA coating was carried out by immersing substrates in a buffer solution (2 mg of dopamine hydrochloride per 1 mL of 10 mM Tris, pH 8.5) at room temperature for 1 h (Lee et al., 2007). The coated substrates were rinsed with deionized water and dried under a stream of nitrogen gas.

2.2.3 Tannic acid (TA) deposition

To deposit TA, the pDA-coated substrates were transferred to ethanolic solutions of FeCl_3 (10 mM) and TA (10 mM). The following cycle was generally used for TA deposition on the pDA-coated surface: (1) FeCl_3 for 1 s, (2) rinsing with ethanol, (3) TA for 1 s, and (4) rinsing with ethanol. Further experiments were carried out after 5 repetitive treatments with FeCl_3 and TA.

2.2.4 PEGylation

PEG was grafted to the pDA-coated and pDA/TA-coated surfaces by incubating the solid substrates in an acidic solution of PEG (1 mg/mL, 0.01 mM HCl) for 10 min. The resulting substrates were rinsed with deionized water and

dried under a stream of nitrogen gas.

2.2.5 Protein adsorption

For the protein adsorption study, nontreated, pDA-, pDA/PEG-, pDA/TA-, and pDA/TA/PEG-coated surfaces were incubated in a PBS buffer solution of fibrinogen (0.1 mg/mL). After 1 h, the substrates were washed with distilled water and dried under a stream of nitrogen gas.

2.2.6 Diatom adhesion

Amphora coffeaeformis was received from the Korea Marine Microalgae Culture Center (KMMCC) and grown in 100 mL of f/2 culture medium at 18 °C for 10 days. The cell suspension (13 mL) was added to Petri dishes containing the solid substrates, and after 1 day at room temperature, the substrates were washed in seawater to remove cells that had not attached to the solid substrates. The attached cells were characterized and counted by optical microscopy (Nikon, LV100ND).

2.2.7 Characterization

X-ray photoelectron spectroscopy (XPS) was carried out using a MultiLab 2000 (Thermo VG Scientific) with a Mg K α X-ray source and ultrahigh vacuum

($\sim 10^{-10}$ mbar). The thickness of the organic layers on the solid substrates was measured using a M-2000D ellipsometer (J.A. Woollam Co.). Static water contact angle measurements were carried out using a Phoenix-300 TOUCH goniometer (Surface Electro Optics Co., Ltd.). Fourier transform infrared spectroscopy (FT-IR) was carried out in single reflection mode using a dry N₂-purged Thermo Nicolet Nexus FT-IR spectrophotometer equipped with the smart SAGA (smart apertured grazing angle) accessory. The *p*-polarized light was incident at 80° relative to the surface normal of the substrate, and a narrow band mercury–cadmium–telluride (MCT) detector cooled with liquid nitrogen was used to detect the reflected light.

2.3 Results and Discussion

The preparation of the marine antifouling surface coating was carried out using a three-step procedure: (1) pDA coating, (2) Fe^{III}-mediated TA deposition (Fe^{III}-TA), and (3) PEGylation resulting in pDA-, pDA/TA-, and pDA/TA/PEG-coated surfaces, respectively (Figure 2.1). Recently, Caruso and coworkers successfully deposited TA layers on solid substrates (Ejima et al., 2013) and also reported that the grafting precursor layers, polyethylenimine, enhanced the adhesion of TA on the substrates (Rahim et al., 2014). However, applications of the approach would

be limited because the adhesion mechanism of the first TA layer on solid substrates has not been fully understood, yet. This drawback encouraged us to develop a well-defined strategy for depositing TA on the substrates. We reported the pDA-assisted TA deposition on solid substrates, where the first TA layer was interacted with the pDA-coated surface by Fe^{III} coordination reaction between the pDA catechol moieties and TA (Kim et al., 2014). Herein, we demonstrated the formation of TA layers on solid substrates using the pDA-assisted strategy. PEGylation of the pDA/TA-coated surface was carried out by immersing the surface into a solution containing PEG. From the various types of available PEG molecules, we chose to use the four-arm PEG because the branched structure of this molecule was expected to be advantageous for hydrogen bond formation. The modifications of the surface by pDA, TA, and PEG were directly characterized by XPS and FT-IR.

For the XPS and FT-IR analyses, Si and Au substrates were used, respectively. In the XPS analysis, the pDA-coated surfaces showed C 1s, N 1s, O 1s, and Si 2p peaks, of which the C 1s and N 1s peaks corresponded to pDA (Figure 2.2a). After treatment with Fe^{III} -TA, new Fe 2p peaks were apparent (Figure 2.2b), and those peaks were decreased after PEGylation, with a concurrent increase in the peak intensities of C 1s and O 1s, corresponding to PEG (Figure 2.2c). The quantitative analysis of the surface chemical composition is shown in Table 2.1. The sequential decrease of the N 1s and Si 2p peaks and increase of the C 1s and

O 1s peaks indicated the successful deposition of TA and PEG on the pDA-coated surface. The C/O ratio for the pDA/TA-coated surface was calculated to be 1.62, which is in good agreement with the theoretical C/O ratio for TA ($C_{76}H_{52}O_{46}$, C/O = 1.65). An XPS narrow scan of the C 1s region also supported the presence of TA and PEG on the pDA-coated surface. The intensities of the peaks at 288.6 eV (C=O) and 286.3 eV (C–O) were significantly increased after TA deposition and PEGylation, respectively (Figure 2.3). These peaks are due to the abundant amount of ester and ether groups in TA and PEG, and these results indicated the successful introduction of TA and PEG onto the surface. FT-IR spectra also revealed the successful modification of the pDA-coated surface by TA and PEG. The pDA-coated surface afforded several characteristic peaks, including ring stretching in benzene ($1500\text{--}1600\text{ cm}^{-1}$), NH_2 deformation (1620 cm^{-1}), C–O and C–N stretching ($1000\text{--}1120\text{ cm}^{-1}$), and NH and OH stretching ($3000\text{--}3500\text{ cm}^{-1}$) (Figure 2.4a) (Kang et al., 2012). Upon TA deposition, a significant increase in the peak intensity in the $900\text{--}1140\text{ cm}^{-1}$ region (C–O stretching) was observed, originating from the surface-deposited TA (Figure 2.4b). Furthermore, peaks originating from ring stretching in benzene ($1500\text{--}1600\text{ cm}^{-1}$) were observed owing to the benzene moieties of TA (Kim et al., 2015). In the pDA/TA/PEG-coated sample, an increase in the peaks for CH antisymmetric and symmetric stretching ($2830\text{--}3000\text{ cm}^{-1}$) and a decrease in the peaks for ring stretching in benzene were detected (Figure 2.4c). All these observations

indicated that TA deposition and PEGylation occurred successfully on the pDA-coated surface.

Prior to use of the pDA/TA/PEG-coated surface for marine antifouling applications, a protein adsorption experiment was carried out. PEG is well-known to effectively inhibit nonspecific protein adsorption (Harris, 1992), and therefore, the functional properties of a surface-grafted PEG can be verified by simple protein adsorption tests. In this study, fibrinogen, which is known to be a sticky protein, was used (Slack et al., 1987), and the amount of adsorbed protein was characterized by spectroscopic ellipsometry. A noticeable protein adsorption was not observed after immersion of the pDA/TA/PEG-coated surfaces in a PBS solution of fibrinogen (0.1 mg/mL, pH 7.4), whereas protein layers of more than 2.7 nm thickness were adsorbed on the nontreated, pDA-, and pDA/TA-coated surfaces (Figure 2.5). As a control, PEGylation was also carried out on the pDA-coated surface without deposited TA, and the resulting surface had a 1.3 nm thick adsorbed protein layer. These results implied that the combined coating of pDA and TA (i.e., pDA/TA coating) is an effective platform for the PEGylation. Based on the fact that surface-grafted PEG functioned well against protein adsorption, marine antifouling experiments were carried out.

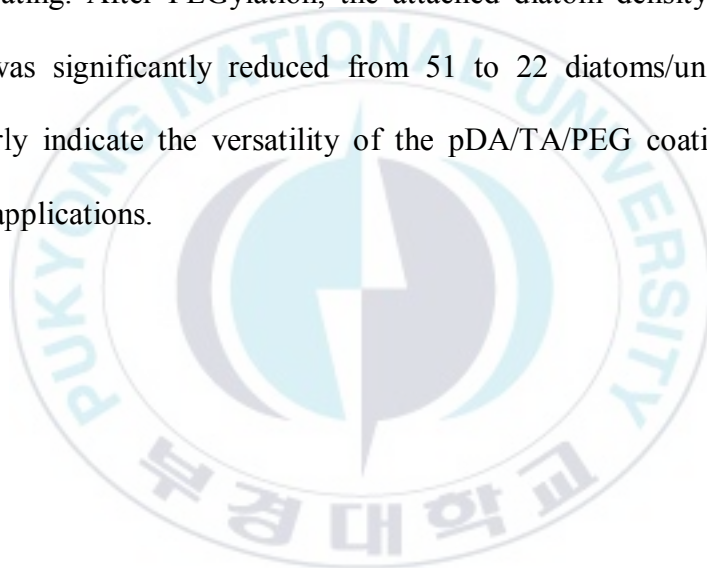
For the marine antifouling experiments, stainless steel was used as a model substrate because stainless steel is the major element of the bodies of marine vessels, on which marine organisms heavily adhere. To characterize the marine

antifouling properties of the coated surfaces, the adhesion behavior of marine diatoms was studied. As a model diatom, *A. coffeaeformis*, which has been frequently utilized in laboratory assays, was selected (Zhu et al., 2013; Holland et al., 2004), cultured in f/2 medium for 10 days, and used for the adhesion assay (concentration of chlorophyll a = 1.1 µg/mL). Figure 2.6 shows the attached diatom density on different coatings after being cultured for 1 day. The diatom densities on the coated surfaces were lower than on the nontreated stainless steel surface. Quantitatively, the pDA, pDA/TA, and pDA/TA/PEG coatings reduced diatom adhesion by 23.6%, 49.7%, and 83.4%, respectively, compared with the nontreated stainless steel. It was interesting that the pDA and pDA/TA coatings (without PEGylation) were also resistant against diatom adhesion. The results were thought to originate from the increased hydrophilicity of the surfaces. It is known that diatom adhesion can be reduced by enhancement of surface hydrophilicity (Schilp et al., 2007; Finlay et al., 2002; Bowen et al., 2007). Considering that the surface hydrophilicity of stainless steel was sequentially increased by the pDA and pDA/TA coatings, the improved hydrophilicity resulted in the reduction of diatom adhesion on the surfaces. The water contact angle of stainless steel was changed from 53.4° to 32.4° and 28.4° after introduction of the pDA and pDA/TA coatings, respectively (Figure 2.7). In particular, the pDA/TA/PEG-coated surfaces showed the most effective antifouling performance, in which less than 20 diatoms/unit area (0.11 mm²) were

attached to the surfaces. As a control, the diatom adhesion test was conducted on the pDA/PEG-coated surface without deposited TA, in order to investigate the effect of TA layers on the PEGylation. As shown in Figure 2.6, a significant improvement of antifouling performance was not observed on the pDA/PEG-coated surfaces. This result indicated that the TA layers play an important role in efficient surface PEGylation.

To evaluate the long-term marine antifouling performance of the coating, the pDA/TA/PEG-coated surfaces were pretreated with filtered seawater. After immersion for 3, 6, and 10 days in seawater, the pDA/TA/PEG-coated surfaces were taken out and the 1 day diatom adhesion assay was then carried out. The attached diatom density was quantified, and the results are shown in Figure 2.8. After 3 days, the resistance against diatom adhesion was similar to that of the as-prepared PEG-coated surfaces. However, after 6 and 10 days of immersion in seawater, the attached diatom density on the PEG-coated surfaces was considerably increased (6 days: 30 diatoms/unit area, 10 days: 42 diatoms/unit area), indicating that the antifouling performance of the PEG-coated surfaces was reduced in seawater. The long-term instability of the pDA/TA/PEG coating on exposure to seawater may be explained by the dissociation of hydrogen bonds between TA and PEG. Gradual cleavage of the hydrogen bonds would cause a decrease in the fouling resistance with time, followed by an increase in diatom adhesion.

The advantage of our PEGylation approach is that diverse materials can be modified. In order to investigate the versatility of the pDA/TA/PEG coating, we choose an additional substrate, nylon, which is frequently utilized for the preparation of aquaculture instruments, applied our approach to modify the surfaces, and carried out marine antifouling experiments. Figure 2.9 shows that PEGylation was also successfully achieved on the nylon surfaces, by virtue of the pDA/TA coating. After PEGylation, the attached diatom density on the nylon substrates was significantly reduced from 51 to 22 diatoms/unit area. These results clearly indicate the versatility of the pDA/TA/PEG coating for marine antifouling applications.



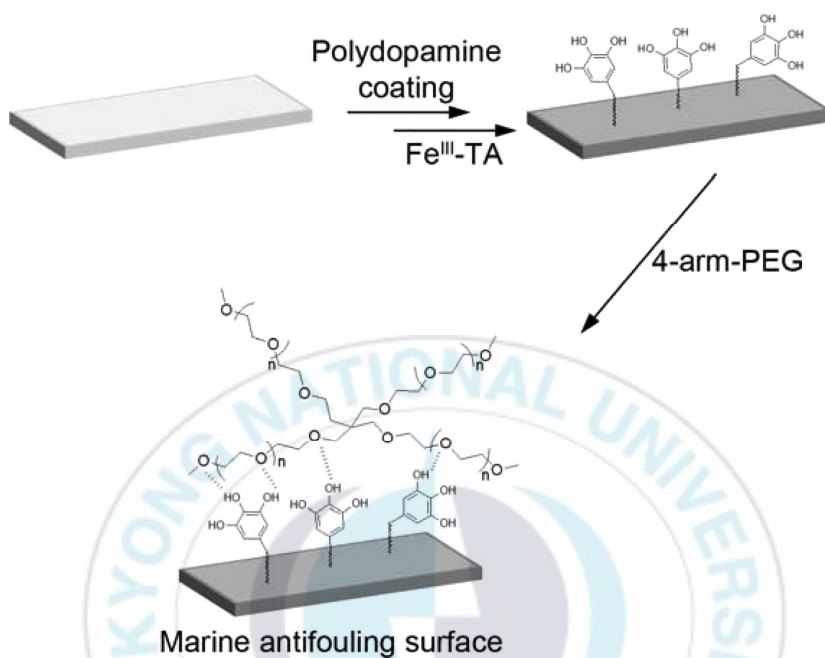


Figure 2.1 Schematic illustration of the preparation of the marine antifouling surface coating.

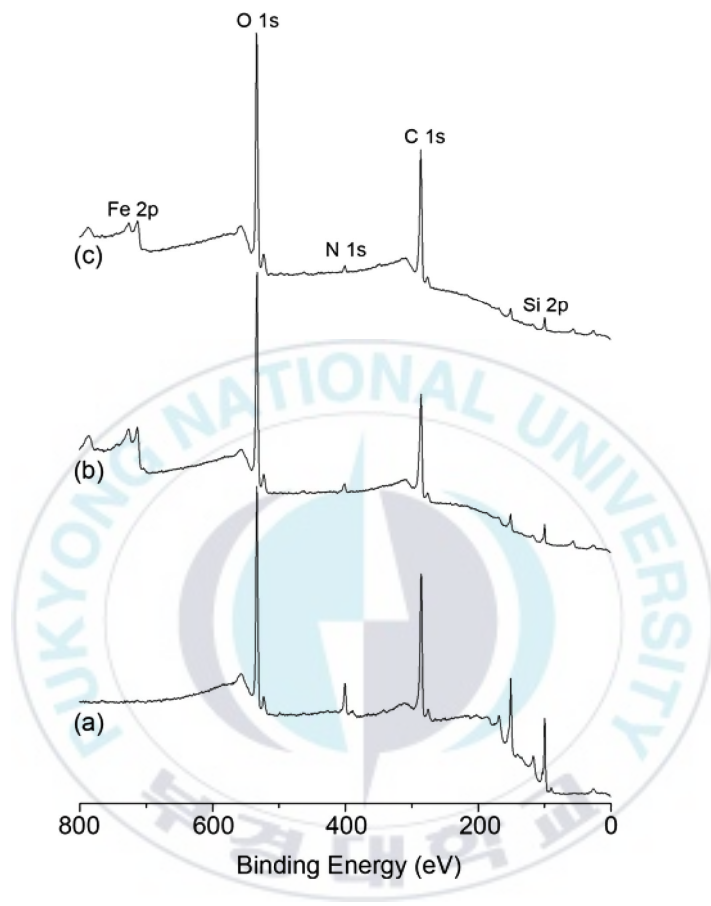
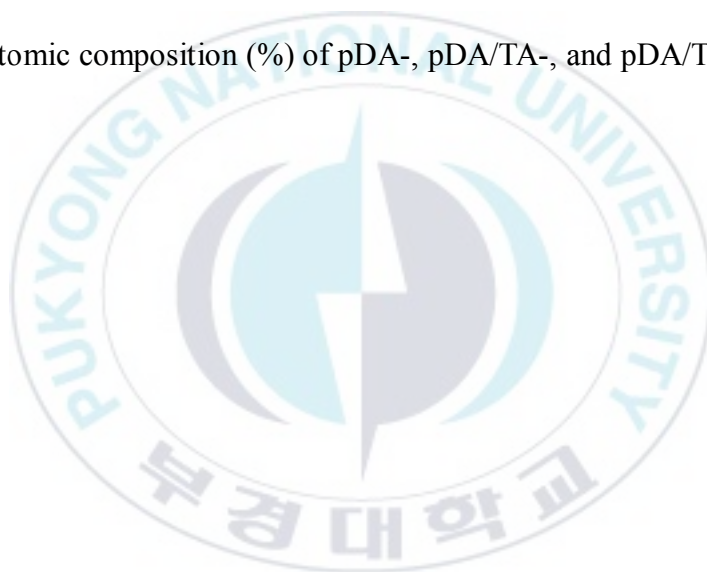


Figure 2.2 X-ray photoelectron spectra of (a) pDA-coated, (b) pDA/TA-coated, and (c) pDA/TA/PEG-coated Si surfaces.

	C 1s	N 1s	O 1s	Fe 2p	Si 2p
pDA	50.68	5.96	22.34	0	21.02
pDA/TA	53.33	2.46	32.92	3.71	7.58
pDA/TA/PEG	58.68	1.8	33.48	1.86	4.17

Table 2.1 Atomic composition (%) of pDA-, pDA/TA-, and pDA/TA/PEG-coated Si surfaces.



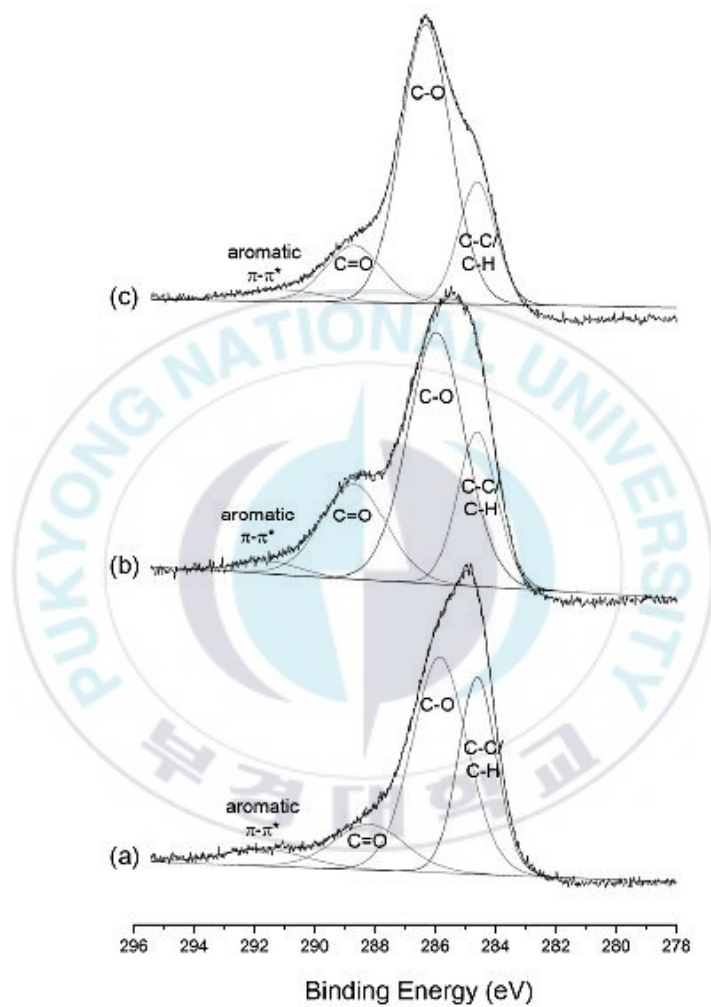


Figure 2.3 High-resolution XPS spectra (C 1s) of (a) pDA-, (b) pDA/TA-coated, and (c) pDA/TA/PEG-coated Si surfaces.

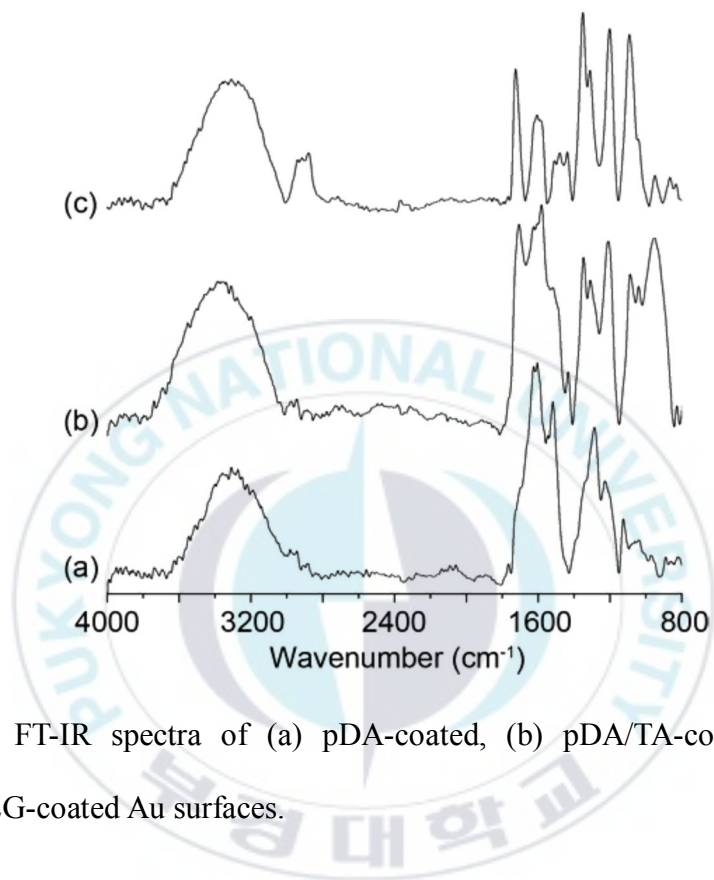


Figure 2.4 FT-IR spectra of (a) pDA-coated, (b) pDA/TA-coated, and (c) pDA/TA/PEG-coated Au surfaces.

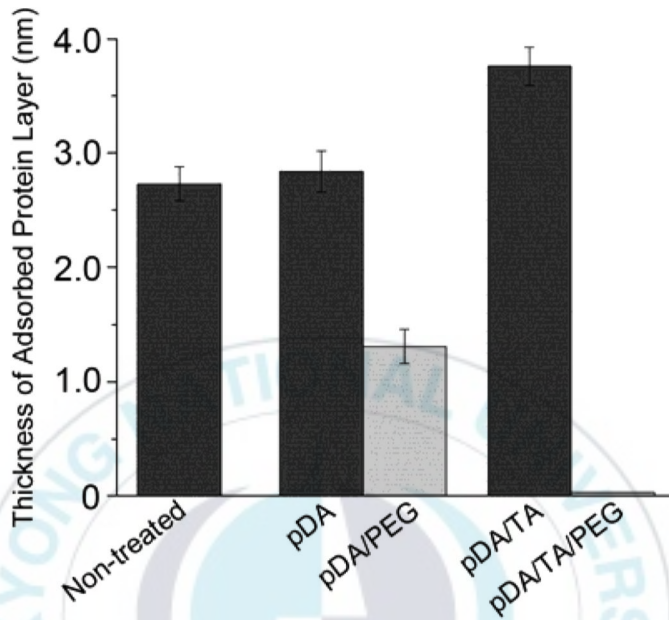


Figure 2.5 Protein adsorption on the different coatings (substrate: Si). Each point is the mean from 15 measurements on 3 replicate samples. The error bars display the 95% confidence limits.

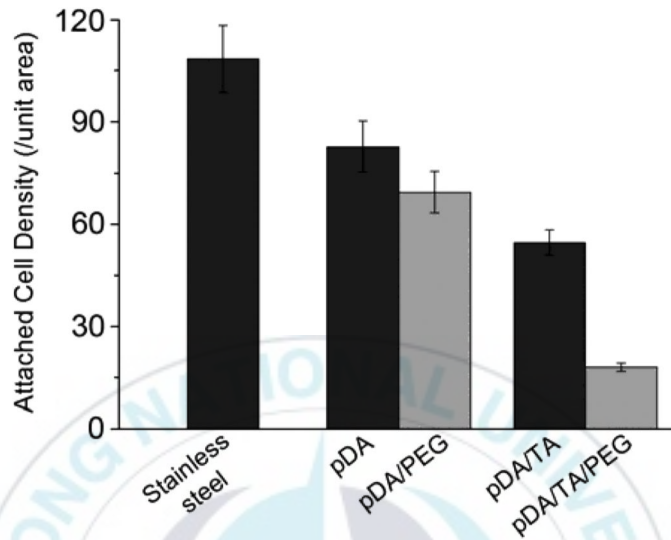


Figure 2.6 Diatom adhesion on the different coatings (substrate, stainless steel; unit area, 0.11 mm²). Each point is the mean from 60 counts on 3 replicate samples. The error bars display the 95% confidence limits.



Figure 2.7 Water contact angle images of (a) non-treated, (b) pDA-, and (c) pDA/TA-coated stainless steel surfaces.

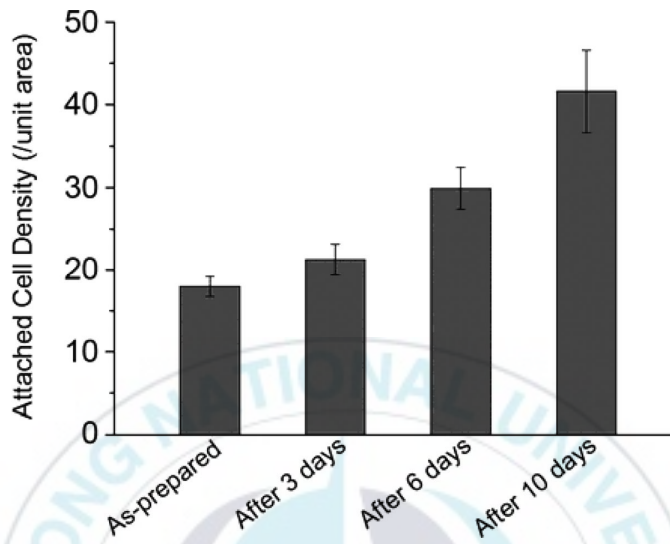


Figure 2.8 Stability of the pDA/TA/PEG coating in seawater (substrate: stainless steel, unit area: 0.11 mm²). Each point is the mean from 60 counts on 3 replicate samples. The error bars display the 95% confidence limits.

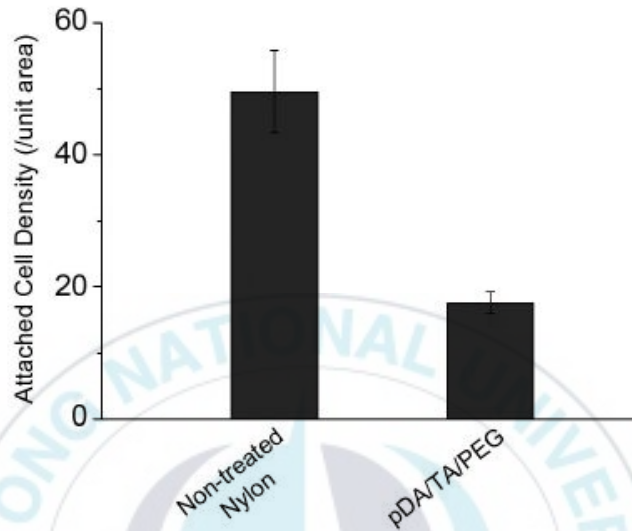


Figure 2.9 Diatom adhesion on non-treated and pDA/TA/PEG-coated nylon surfaces (unit area: 0.11 mm²). Each point is the mean from 60 counts on 3 replicate samples. The error bars display the 95% confidence limits.

2.4 Conclusions

In summary, a facile approach to the preparation of marine antifouling surface coatings was developed using TA and PEG. TA is known to be a good PEG-binding agent, and was successfully deposited on the solid substrates via a metal coordination reaction. Subsequent PEGylation was achieved by hydrogen bond formation. This approach has several advantages; the whole process proceeds under mild reaction conditions without complicated steps or instruments. Remarkably, only simple immersion of the substrate into the reagent containing solutions was required to prepare the marine antifouling surface coatings. Moreover, the versatility of the investigated method was confirmed by applying this method to both polymer and metal alloy substrates. Unlike the nontreated surfaces, diatom adhesion was significantly inhibited on the modified surfaces. Given the environmentally friendly processing conditions and the practical applicability of this method, we believe that this method provides an important alternative approach to the previously developed antifouling coatings for marine vessels.

2.5. References

Bowen, J.; Pettitt, M. E.; Kendall, K.; Leggett, G. J.; Preece, J. A.; Callow, M. E.; Callow, J. A. **2007**. The Influence of Surface Lubricity on the Adhesion of *Navicula perminuta* and *Ulva linza* to Alkanethiol Self-Assembled Monolayers. *J. R. Soc. Interface* 4: 473-477.

Callow, J. A.; Callow, M. E. In *Biological Adhesives*; Smith, A. M.; Callow, J. A., Eds.; Springer: New York, 2006; pp 63-78.

Callow, J. A.; Callow, M. E. **2011**. Trends in the Development of Environmentally Friendly Fouling-Resistant Marine Coatings. *Nat. Commun.* 2: 244.

Cho, Y.; Sundaram, H. S.; Weinman, C. J.; Paik, M. Y.; Dimitriou, M. D.; Finlay, J. A.; Callow, M. E.; Callow, J. A.; Kramer, E. J.; Ober, C. K. **2011**. Triblock Copolymers with Grafted Fluorine-Free, Amphiphilic, Non-ionic Side Chains for Antifouling and Fouling-Release Applications. *Macromolecules* 44: 4783-4792.

Ejima, H.; Richardson, J. J.; Liang, K.; Best, J. P.; van Koeveden, M. P.; Such, G. K.; Cui, J.; Caruso, F. **2013**. One-Step Assembly of Coordination Complexes for

Versatile Film and Particle Engineering. *Science* 341: 154-157.

Ekblad, T.; Bergstrom, G.; Ederth, T.; Conlan, S. L.; Mutton, R.; Clare, A. S.; Wang, S.; Liu, Y.; Zhao, Q.; D'Souza, F.; Donnelly, G. T.; Willemsen, P. R.; Pettitt, M. E.; Callow, M. E.; Callow, J. A.; Liedberg, B. **2008**. Poly(ethylene glycol)-Containing Hydrogel Surfaces for Antifouling Applications in Marine and Freshwater Environments. *Biomacromolecules* 9: 2775-2783.

Finlay, J. A.; Callow, M. E.; Ista, L. K.; Lopez, G. P.; Callow, J. A. **2002**. The Influence of Surface Wettability on the Adhesion Strength of Settled Spores of the Green Alga *Enteromorpha* and the Diatom *Amphora*. *Integr. Comp. Biol.* 42: 1116-1122.

Harris, J. M. **1992**. Introduction to Biotechnical and Biomedical Applications of Poly(ethylene glycol); *Springer*: New York.

Holland, R.; Dugdale, T. M.; Wetherbee, R.; Brennan, A. B.; Finlay, J. A.; Callow, J. A.; Callow, M. E. **2004**. Adhesion and Motility of Fouling Diatoms on a Silicone Elastomer. *Biofouling* 20: 323-329.

Jones, D. E. **1965**. Banana Tannin and Its Reaction with Polyethylene Glycols.

Nature 206: 299-300.

Kang, S. M.; Hwang, N. S.; Yeom, J.; Park, S. Y.; Messersmith, P. B.; Choi, I. S.; Langer, R.; Anderson, D. G.; Lee, H. **2012**. One-Step Multipurpose Surface Functionalization by Adhesive Catecholamine. *Adv. Funct. Mater.* 22: 2949-2955.

Kim, S.; Kim, D. S.; Kang, S. M. **2014**. Reversible Layer-by-Layer Deposition on Solid Substrates Inspired by Mussel Byssus Cuticle. *Chem.-Asian J.* 9: 63-66.

Kim, S.; Kwak, S.; Lee, S.; Cho, W. K.; Lee, J. K.; Kang, S. M. **2015**. One-Step Functionalization of Zwitterionic Poly[(3-(methacryloylamino)propyl)dimethyl (3-sulfopropyl)ammonium hydroxide] Surfaces by Metal-Polyphenol Coating. *Chem. Commun.* 51: 5340-5342.

Lee, H.; Dellatore, S. M.; Miller, W. M.; Messersmith, P. B. **2007**. Mussel-Inspired Surface Chemistry for Multifunctional Coatings. *Science* 318: 426-430.

Lejars, M.; Margaille, A.; Bressy, C. **2012**. Fouling Release Coatings: A Nontoxic Alternative to Biocidal Antifouling Coatings. *Chem. Rev.* 112: 4347-4390.

Park, D.; Weinman, C. J.; Finlay, J. A.; Fletcher, B. R.; Paik, M. Y.; Sundaram, H. S.; Dimitriou, M. D.; Sohn, K. E.; Callow, M. E.; Callow, J. A.; Handlin, D. L.; Willis, C. L.; Fischer, D. A.; Kramer, E. J.; Ober, C. K. **2010**. Amphiphilic Surface Active Triblock Copolymers with Mixed Hydrophobic and Hydrophilic Side Chains for Tuned Marine Fouling-Release Properties. *Langmuir* 26: 9772-9781.

Pettitt, M. E.; Henry, S. L.; Callow, M. E.; Callow, J. A.; Clare, A. S. **2004**. Activity of Commercial Enzymes on Settlement and Adhesion of Cypris Larvae of the Barnacle *Balanus Amphitrite*, Spores of the Green Alga *Ulva llinza*, and the Diatom *Navicula perminuta*. *Biofouling* 20: 299-311.

Rahim, M. A.; Ejima, H.; Cho, K. L.; Kempe, K.; Mullner, M.; Best, J. P.; Caruso, F. **2014**. Coordination-Driven Multistep Assembly of Metal-Polyphenol Films and Capsules. *Chem. Mater.* 26: 1645-1653.

Schilp, S.; Kueller, A.; Rosenhahn, A.; Grunze, M.; Pettitt, M. E.; Callow, M. E.; Callow, J. A. **2007**. Settlement and Adhesion of Algal Cells to Hexa(ethylene glycol)-Containing Self-Assembled Monolayers with Systematically Changed Wetting Properties. *Biointerphases* 2: 143-150.

Schofield, P.; Mbugua, D. M.; Pell, A. N. **2001**. Analysis of Condensed Tannins: A Review. *Anim. Feed Sci. Technol.* *91*: 21-40.

Sileika, T. S.; Barrett, D. G.; Zhang, R.; Lau, K. H. A.; Messersmith, P. B. **2013**. Colorless Multifunctional Coatings Inspired by Polyphenols Found in Tea, Chocolate, and Wine. *Angew. Chem., Int. Ed.* *52*: 10766-10770.

Slack, S. M.; Bohnert, J. L.; Horbett, T. A. **1987**. The Effects of Surface Chemistry and Coagulation Factors on Fibrinogen Adsorption from Plasma. *Ann. N. Y. Acad. Sci.* *516*: 223-243.

Statz, A.; Finlay, J.; Dalsin, J.; Callow, M.; Callow, J. A.; Messersmith, P. B. **2006**. Algal Antifouling and Fouling-Release Properties of Metal Surfaces Coated with a Polymer Inspired by Marine Mussels. *Biofouling* *22*: 391-399.

Umemura, K.; Yamada, T.; Maeda, Y.; Kobayashi, K.; Kuroda, R.; Mayama, S. **2007**. Regulated Growth of Diatom Cells on Self-Assembled Monolayers. *J. Nanobiotechnol.* *5*: 2.

Wan, F.; Pei, X.; Yu, B.; Ye, Q.; Zhou, F.; Xue, Q. **2012**. Grafting Polymer Brushes on Biomimetic Structural Surfaces for Anti-algae Fouling and Foul

Release. *ACS Appl. Mater. Interfaces* 4: 4557-4565.

Wan, F.; Ye, Q.; Yu, B.; Pei, X.; Zhou, F. **2013**. Multiscale Hairy Surfaces for Nearly Perfect Marine Antibiofouling. *J. Mater. Chem. B* 1: 3599-3606.

Weinman, C. J.; Finlay, J. A.; Park, D.; Paik, M. Y.; Krishnan, S.; Sundaram, H. S.; Dimitriou, M.; Sohn, K. E.; Callow, M. E.; Callow, J. A.; Handlin, D. L.; Willis, C. L.; Kramer, E. J.; Ober, C. K. **2009**. ABC Triblock Surface Active Block Copolymer with Grafted Ethoxylated Fluoroalkyl Amphiphilic Side Chains for Marine Antifouling/Fouling-Release Applications. *Langmuir* 25: 12266-12274.

Wetherbee, R.; Lind, J. L.; Burke, J.; Quatrano, R. S. **1998**. The First Kiss: Establishment and Control of Initial Adhesion by Raphid Diatoms. *J. Phycol.* 34: 9-15.

Yebra, D. M.; Kiil, S.; Dam-Johansen, K. **2004**. Antifouling Technology-Past, Present and Future Steps Towards Efficient and Environmentally Friendly Antifouling Coatings. *Prog. Org. Coat.* 50: 75-104.

Zhang, Z.; Finlay, J. A.; Wang, L.; Gao, Y.; Callow, J. A.; Callow, M. E.; Jiang, S. **2009**. Polysulfobetaine-Grafted Surfaces as Environmentally Benign Ultralow

Fouling Marine Coatings. *Langmuir* 25: 13516-13521.

Zhu, X.; Jan.czewski, D.; Lee, S. S. C.; Teo, S. L.-M.; Vancso, G. J. **2013**. Cross-Linked Polyelectrolyte Multilayers for Marine Antifouling Applications. *ACS Appl. Mater. Interfaces* 5: 5961-5968.



Chapter 3. Construction of Anti-Bacterial Alginate Films using Catechol-Fe(III) Interactions

3.1 Introduction

The development of antifouling surface coatings has gained a great deal of attention, because biofouling on synthetic surfaces cause serious problem (Banerjee et al., 2011). The non-specific adsorption of protein, bacteria and cells at biomaterial surfaces gives rise to adverse effects such as bacterial infection and other undesirable responses (Castner et al., 2002; Page et al., 2009). Therefore, much effort has been made to inhibit biofouling, and poly(ethylene glycol) (PEG), zwitterionic polymer, and polysaccharide coatings have been utilized (Unsworth et al., 2005; Kingshott et al., 2003; Caro et al., 2009; Cheng et al., 2007; Cho et al., 2007; McLean et al., 2000; Martwiset et al., 2006; Liu et al., 2014; Lee et al., 2007). Among them, polysaccharides have been frequently used for inhibiting protein and cell adsorption, due to their excellent hydrophilic property (Morra et al., 1999; McArthur et al., 2000). Hydrophilic polysaccharides interact with water and result in hydration layer.

Especially, alginate, an anionic polysaccharide typically extracted from brown algae, is of interest as an antifouling material (Karbassi et al., 2014; Lee and

Mooney, 2012). Alginate has a (1-4)-linkage between β -D-mannuronic acid and α -L-guluronic acid residues (Wen and Oh, 2014), and carboxylic acid groups contained in the alginate were successfully utilized for surface functionalization (Morra and Cassinelli, 1998; 1999; Yoshioka et al; 2003). For example, Morra et al. showed that surface-immobilized alginate effectively reduce the adhesion of fibroblast cells. Yoshioka et al. also used alginate for preventing platelet adsorption. Alginate was grafted to stainless steel surface via amide bond forming reaction, and platelet adhesion was found to be significantly reduced on the alginate-immobilized surface. Although the antifouling surface coating was successfully conducted using alginate, the method is not applicable to various types of materials, and thus, the development of versatile alginate surface coatings is required.

The mussel, a famous marine fouling organisms, secretes adhesive proteins and attach to virtually any material surfaces (Waite and Tanzer, 1981). In particular, catechol moieties of unusual amino acid 3,4-dihydroxy-L-phenylalanine (DOPA) in the adhesive proteins were revealed to be crucial component in mussel adhesion (Waite, 1999; Waite et al., 2001). Thus, mussel-inspired polymers have been functionalized with catechol which has been extensively studied as surface modification (Faure et al., 2012).

For this reason, various anti-fouling polymers were conjugated with catechol, and successfully used in the material-independent surface coatings (Lee et al.,

2010; Park et al., 2013; You et al., 2011). For instance, Park et al. synthesized a catechol-conjugated dextran to coat titania surface, and showed that cell adhesion was effectively reduced on the dextran-coated surface. Recently, Lee et al. reported that the catechol-grafted poly (ethylene glycol) (PEG) backbone could be immobilized on various material substrates including noble metals, metal oxides, and synthetic polymers. The resulting PEGylated surfaces showed effectively preventing serum proteins and cell adhesion. Furthermore, You et al. synthesized catechol-conjugated heparin compounds that are adherent to poly urethane substrate, and observed that blood coagulation and platelet adhesion was significantly reduced on the heparin-coated surfaces.

In this study, we report that catechol-conjugated alginates are advantageous for the anti-bacterial surface preparation. Catechol-conjugated alginates were synthesized using an amide bond forming reaction, and the resultant was introduced on the surface via iron (III) coordination reaction. To test the antibacterial property of the surface, *E. coli* cells were used, and ultra-low adhesion of bacteria was observed.

3.2 Experimental Section

3.2.1 Materials

Dopamine hydrochloride (98%, Aldrich), alginic acid sodium salt (low viscosity, Alfa Aesar), *N*-hydroxysuccinimide (NHS 98+%, Alfa Aesar), 1-(3-dimethylaminopropyl)-3-ethylcarbodiimide hydrochloride (EDC, TCI), phosphate buffered saline tablet (Sigma-Aldrich), sodium phosphate dibasic heptahydrate (99%, Sigma-Aldrich), sodium phosphate monobasic dihydrate (98%, Sigma-Aldrich), trizma base (99%, Sigma), trizma HCl (99%, Sigma), iron(III) chloride hexahydrate ($\text{FeCl}_3 \cdot 6\text{H}_2\text{O}$, 97%, Sigma-Aldrich), fibrinogen (from human plasma, Sigma), hydrochloric acid (HCl, 35~37%, Duksan), sodium hydroxide (NaOH, 93%, Duksan), EDTA (0.5 M, pH 8.0, Mentos), Luria-Bertani (LB, containing 5 g Yeast Extract, BD Biosciences), tryptone (LPS solution), sodium chloride (Calbiochem), and Live/Dead BacLight™ bacterial viability kit (L-13152, Molecular Probes) were used as received. LB broth was prepared by mixing LB with 10 g of tryptone and 10 g of sodium chloride in 1 L of deionized water.

3.2.2 Synthesis of Catechol-Conjugated Alginates (Alg-C)

Alginate (1 g) was dissolved in sodium phosphate buffer (SPB) (0.1 M, pH 6.0, 100 mL). EDC (1.63 g) and NHS (0.98 g) were dissolved in the SPB solution (20 mL) and subsequently added to the alginate solution to activate the carboxylic acid groups in alginate. The solution was stirred at room temperature for 20 min, and dopamine solution (0.5 g in 20 mL of SPB) was added to the activated alginate solution. The resulting mixture was stirred at room temperature for

additional 9 h. The solution was transferred to a dialysis membrane (MWCO = 3500 Da) and dialyzed for 48 h to remove unreacted coupling reagents and dopamine. Acidified water (1 mL addition of 5 M HCl per 1 L of distilled water) was used during the dialysis step. The final product was freeze-dried and kept in a refrigerator.

3.2.3 Polydopamine (pDA) Coating

Si/SiO₂ substrates (1 cm × 1 cm) were cleaned in acetone and ethanol with sonication prior to use. pDA coating was performed by immersing substrates in a buffer solution (2 mg of dopamine hydrochloride per 1 mL of 10 mM Tris, pH 8.5) at room temperature for 1 h. The coated substrates were rinsed with deionized water and dried under a stream of nitrogen gas.

3.2.4 Spin-Coating of Alg-C

pDA-coated substrates were transferred to Alg-C and FeCl₃ solution for constructing alginic acid films. Alg-C was deposited on the pDA-coated substrates using following steps: i) a 100 μL of Alg-C solution (1, 2, 5, 10, and 15 mg/mL) was dropped onto the pDA-coated substrates, and the substrates were rotated at 4500 rpm for 30 sec, ii) spin-coated substrates were then immersed in the solution of FeCl₃ (0.1 M), iii) After 1-h immersion, the resulting substrates

were taken out, rinsed with deionized water, and dried in a stream of nitrogen gas, iv) finally, Fe^{III}-treated Alg-C was incubated in a buffer solution (10 mM PBS, pH 7.4) for 1 h to form stable catechol-Fe^{III}-catechol bonds .

3.2.5 Stability Test

To test the chemical stability of the Alg-C layer on pDA-coated solid substrates, the substrates were immersed in alkali (10 mM NaOH), acid (10 mM HCl), and neutral (10 mM PBS, pH 7.4) solutions. After 1-h immersion, substrates were taken out, rinsed with water, and dried under a stream of nitrogen gas. Various control experiments were performed to investigate the effect of Fe^{III} coordination, catechol conjugation, and pDA coating on the formation of Alg layers.

3.2.6 Protein Adsorption Test

For the protein adsorption study, non-treated, pDA-coated, and pDA/Alg-C/Fe^{III}-coated Si/SiO₂ substrates were incubated in a fibrinogen solution (0.1 mg/mL in PBS). After 1 h, the resulting substrates were washed with deionized water and dried under a stream of nitrogen gas.

3.2.7 Antibacterial Test

The antibacterial properties of Alg-C films were investigated against *Escherichia coli* (*E. coli* DH5 α). *E. coli* cells were pre-cultured in liquid LB broth

for 14 h at 37°C and the pre-culture was used to inoculate a sub-culture, which was incubated until an optical density (OD) at 600 nm reached 0.6 using UV/Vis spectrophotometer (Optizen POP; Mecasys Co.). *E. coli* culture was harvested by centrifugation at 2,500 rpm for 20 min and washed with PBS. *E. coli* cells were resuspended in LB broth to a concentration of 1×10^7 cells/mL. The *E. coli* suspension was incubated with various substrates including non-treated substrates for 6 h or 24 h at 37°C. After incubation, the substrates were washed with PBS for 30 min at 37°C to remove any non-adhered or loosely adhered *E. coli* cells, and then were immersed into a dye solution (3 μ M of SYTO 9 and 3 μ M of propidium iodide in PBS) at room temperature under dark environment for 20 min. The images of adherent *E. coli* cells on the substrates were taken by a LSM 700 confocal microscope (Carl Zeiss). The number of adherent *E. coli* cells on each substrate was analyzed by using the open-source software ImageJ (National Institute of Health, Bethesda, MD).

3.2.8 Characterizations

X-ray photoelectron spectra were obtained using a MultiLab 2000 (Thermo VGScientific, UK) with a Mg K X-ray source under ultrahigh vacuum ($\sim 10^{-10}$ mbar). The thickness of organic layers on solid substrates was measured using an M-2000D ellipsometer (J.A. Woollam Co., USA).

3.3 Results and Discussion

Alg-C was synthesized via carbodiimide coupling chemistry (EDC/NHS chemistry) as described in the method section (Figure 3.1a). The activated carboxyl group of alginate by EDC/NHS was reacted to the primary amine group of dopamine, forming an amide bond. The reaction was performed in an SPB solution (pH 6.0) for 9 h, and then dialyzed (MWCO=3500 Da). UV-Vis spectroscopy results confirmed that the conjugation efficiency of dopamine to the Alg was 5.9 %, as determined by absorbance at 280 nm (Figure 3.1b). The absorbance at 280 nm was used to quantify catechol content in the product, Alg-C.

The construction of the anti-bacterial surface using Alg-C was carried out by a three-step procedure: (1) polydopamine (pDA) coating, (2) spin coating of Alg-C, and (3) Fe^{III} coordination reaction, resulting in pDA-, pDA/Alg-C-, and pDA/Alg-C/Fe^{III}-coated Si/SiO₂ surfaces (Figure 3.2). pDA coating, which is a well-known method introducing catechols on solid substrates (Lee et al., 2007), was performed by immersing Si/SiO₂ substrates in an alkaline dopamine solution. Subsequently, spin coating of Alg-C was carried out on the pDA-coated substrates, resulting in pDA/Alg-C-coated substrates. The substrates were then treated using an FeCl₃ solution to make catechol-Fe^{III} coordination bonds between pDA-coated surface and Alg-C. pDA/Alg-C/Fe^{III}-coated substrates were additionally

incubated in a PBS solution (10 mM, pH 7.4) for 1 h to make stable catechol- Fe^{III} -catechol bond formation. The procedure was inspired by the mussel's byssal thread formation. It was known that byssal thread is made by two-step procedure: i) secretion of acidic precursors from the body into the ocean and ii) hardening of byssal thread precursors under alkaline conditions (Holten-Andersen et al., 2011; Yu et al., 2011). Emulating the process of mussel byssus formation, Messersmith et al. reported that mixing catechol-conjugated macromolecules with an acidic solution of Fe^{III} , followed by pH jump from acidic to neutral or alkali resulted in strong hybrid molecules (Messersmith et al., 2013). In this study, we have also mimicked the mussel's byssal thread formation, and as a result, a facile method for the preparation of chemically stable and antibacterial Alg layers was successfully developed.

Si/SiO₂ substrates functionalized by pDA, pDA/Alg-C, and pDA/Alg-C/ Fe^{III} were characterized by x-ray photoelectron spectroscopy and ellipsometry. The X-ray photoelectron spectrum of a pDA-coated substrate showed C 1s, N 1s, O 1s, and Si 2p peaks, of which the C 1s and N 1s peaks corresponded to pDA (Figure 3.3). After the spin coating of Alg-C, the Si substrate peak (Si 2p) disappeared, and the O 1s peak increased from 21.33% to 37.82%, with a concurrent decrease in the peak intensities of C 1s and N 1s (C 1s: 63.94 → 58.66%, N 1s: 6.53 → 3.52%). After treatment with Fe^{III} , new Fe 2p peaks were apparent, and the surface elemental ratio (C/O) was 1.08, which was nearly consistent with that of

Alg (1.0). These results indicated that Alg-C layers were successfully immobilized on the pDA-coated Si/SiO₂ surface. The ellipsometry measurement also confirmed the successful introduction of Alg-C on the pDA-coated surface. Spin coating of Alg-C (15 mg/mL) was carried out on the 10.0- nm-thick pDA layer, and total thickness of the pDA/Alg-C layer was measured to be 69.0 nm, indicating a 59.0-nm-thick Alg-C layer. Thickness of the Alg-C layer was decreased to 37.4 nm during the Fe^{III} treatment and incubation under neutral conditions (pH 7.4). We also found that our approach for constructing Alg-C layers on solid substrates is advantageous for the thickness control. Thickness of Alg-C layers highly depended on the concentration of Alg-C solutions, and Alg-C layers with various thickness were successfully prepared. Specifically, 36.4, 18.6, 10.2, 2.6, and 0.4 nm-thick Alg-C layers were formed on solid substrates using solutions of Alg-C (1, 2, 5, 10, and 15 mg/mL) (Figure 3.4).

To investigate the effect of Fe^{III} coordination on the formation of stable Alg layers on solid substrates, various types of control experiments were designed (Figure 3.5). Firstly, chemical stability of pDA/Alg-C layer was examined by measuring the thickness change upon the chemical treatments. In the case of Fe^{III}-treated samples, pDA/Alg-C layer showed good stability against alkali, acid, and neutral. However, the pDA/Alg-C layer which was untreated by Fe^{III} was significantly detached upon the chemical treatments. It implies that Fe^{III} treatment is important for the formation of chemically stable Alg-C layers. The role of

catechol was also confirmed by using non-treated alginate (Alg). Unlike the pDA/Alg-C layer, pDA/Alg layer (regardless of Fe^{III} treatment) was mostly detached from the surface upon the chemical treatments. These results showed that both catechol conjugation and crosslinking of catechols by Fe^{III} coordination significantly improve the chemical stability of Alg layers on solid substrates.

An interesting feature of our approach for constructing Alg-C films is reversibility. In our approach, the Alg-C layer was cross-linked by Fe^{III}, and thus, the constructed Alg-C layer can be disrupted by removal of Fe^{III}. To demonstrate this, we carried out a simple test, EDTA treatment of Alg-C layers. EDTA is a well-known transition metal chelating agent, and therefore, Fe^{III} contained in Alg-C layers can be removed by an EDTA treatment (Zeng et al., 2010). The prepared pDA/Alg-C/Fe^{III}-coated substrates were immersed in an EDTA solution (pH 8.0, 0.5 M) for 30 min, and the remaining Alg-C layers were characterized by ellipsometry and XPS (Figure 3.6). After treatment with EDTA, the almost Alg-C layer was removed from the surface (30.9 → 1.0 nm) (Figure 3.6a). The X-ray photoelectron spectroscopy also confirmed the detachment of the Alg-C layer. The spectra of EDTA-treated surface displayed no Fe 2p peak and significant increase of N 1s peak which corresponds to underlying pDA (Figure 3.6b). These results clearly showed that Alg-C layer is removable from the surface by an EDTA treatment, and we expect that the reversible control of the Alg-C layer can be applied to the spatio-selective deposition of Alg-C.

The prepared Alg-C layer was expected to show excellent non-biofouling property, because surface-immobilized Alg was known to inhibit fibroblast and platelet adhesion (Morra et al., 1998, 1999; Yoshioka et al., 2003). So, we tested the non-biofouling property of Alg-C layer against protein adsorption and bacteria adhesion. For the protein adsorption test, fibrinogen was chosen as a model protein, samples were immersed into the solution of fibrinogen (0.1 mg/mL, pH 7.4) and the amount of adsorbed protein layer was determined by spectroscopic ellipsometry after 1-h immersion. In the case of non-treated sample, 2.23-nm-thick protein layers were adsorbed on the surface. However, the introduction of Alg-C layer on the surface significantly suppressed protein adsorption (Figure 3.7). Quantitatively, thicknesses of adsorbed protein on the 0.4- and 2.6-nm-thick Alg-C layers were measured to be 1.13 and 0.18 nm, respectively. In particular, noticeable protein adsorption was not observed on the more the 10-nm-thick Alg-C layers. These results indicated the strong resistance of Alg-C layers against protein adsorption, which is adjustable by the thickness control of Alg-C layers.

The antibacterial property of the Alg-C layers was finally examined. To investigate antibacterial effect of the Alg-C layers with various thicknesses, substrates were incubated with *E. coli* (1×10^7 cells/mL) in LB broth. After a certain time of incubation, the substrates were stained with BacLight live/dead dye, which allows us to distinguish viable bacterial cells from dead ones on the basis of their membrane integrity (Figure 3.8). After 6 h, non-treated and pDA-

coated surfaces (i.e., controls) were fully covered with *E. coli* cells (Figure 3.8a and b, upper panel). In contrast, *E. coli* cells adhered significantly less to Alg-C layers with thicknesses of 2.57 nm and 0.44 nm (Figure 3.8f and g, upper panel). Moreover, *E. coli* cells scarcely adhered to Alg-C layers with 10.15 nm or higher (Figure 3.8c-e, upper panel). Quantitatively, the various Alg-C layers of 36.42 nm, 18.59 nm, 10.15 nm, 2.57 nm, and 0.44 nm reduced *E. coli* cell adhesion by 99.92%, 98.98%, 99.80%, 74.07%, and 77.07%, respectively, compared with non-treated surface (Figure 3.9). These results clearly demonstrated that Alg-C layers with more than 10 nm-thickness have the immense antibacterial effect.

The antibacterial capability of Alg-C layers has been preserved even after 24 h (Figure 3.8, lower panel). Noticeable adhesion of *E. coli* cells was not observed on the Alg-C layers with 10.15 nm or higher thicknesses, whereas the bacterial cells adhered more densely to non-treated and pDA-coated surfaces, showing accumulated bacterial layers (Figure 3.8a'-e'). Interestingly, thin Alg-C layer with 2.57 nm was effective enough to suppress bacterial adhesion after 24 h incubation. The layer with 0.44 nm was also able to reduce bacterial adhesion; however, aggregated cells, which could be biofilm further, were observed (Figure 3.8f' and g'). Quantitatively, the various Alg-C layers of 36.42 nm, 18.59 nm, 10.15 nm, 2.57 nm, and 0.44 nm reduced *E. coli* cell adhesion by 99.97%, 99.99%, 100%, 90.36%, and 85.48%, respectively, compared with non-treated surface (Figure 3.9). The pDA-coated surface, however, shows significantly higher bacterial

attachment with 167.53% increase, compared with non-treated surface. This might be related to the fact that pDA could enhance the adsorption of proteins and polysaccharides (Zhu et al., 2011; Wei et al., 2011), which could be produced during bacteria attachment and growth on the surface, resulting in increased bacterial adhesion (Wang et al., 2012). Taken together, the suppression of bacterial attachment onto the surface is exclusively due to the presence of the Alg-C layer.



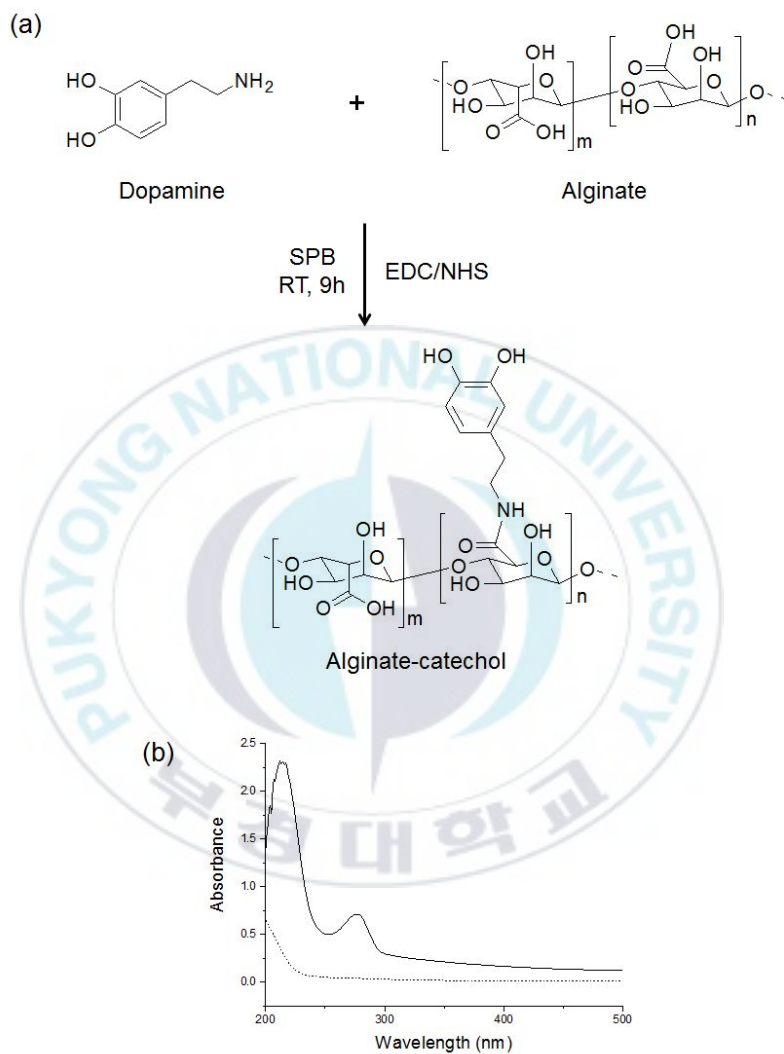


Figure 3.1 (a) A schematic illustration of the synthesis of alginate-catechol. (b) UV-vis spectra of alginate-catechol (1 mg/mL, solid) and alginate (1 mg/mL, dash).

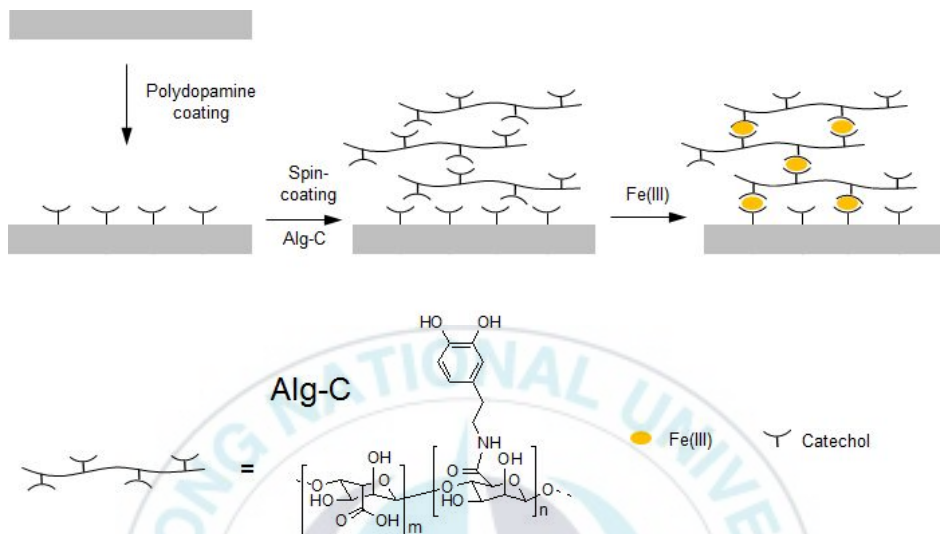


Figure 3.2 Schematic illustration of the preparation of the anti-bacterial surface coating.

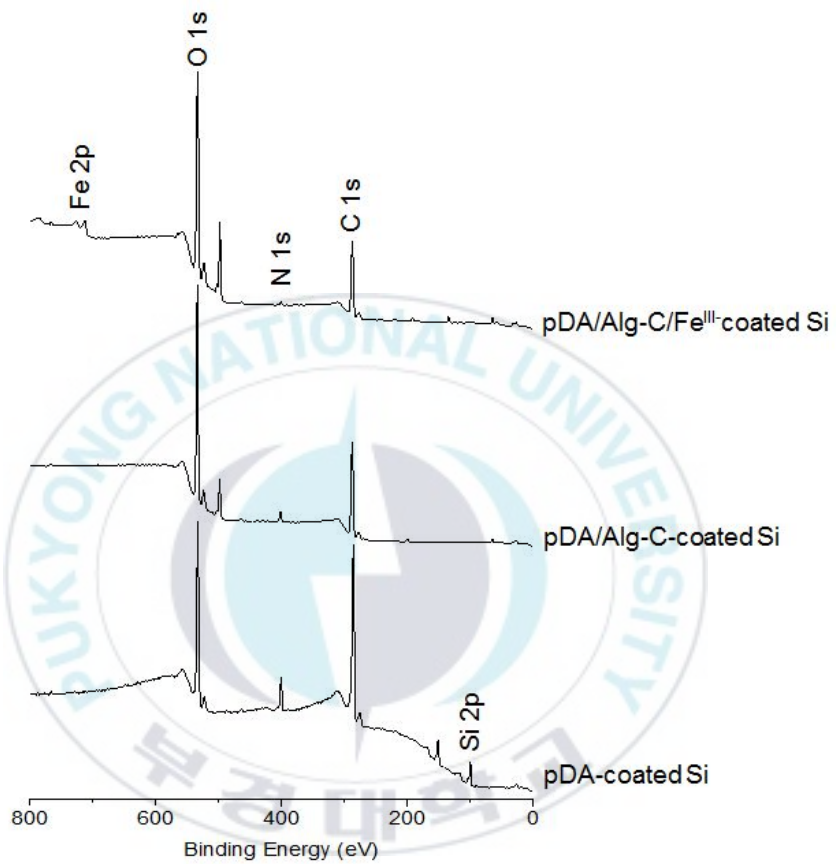


Figure 3.3 X-ray photoelectron spectra of different coatings.

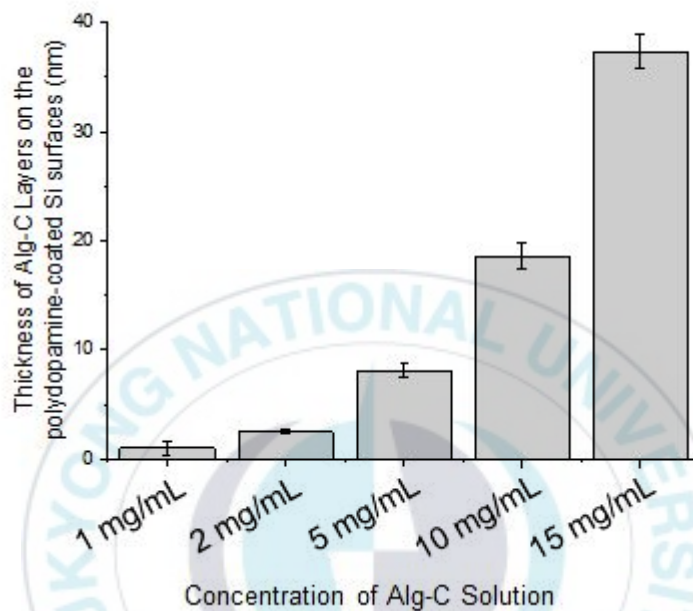


Figure 3.4 Thickness of Alg-C layer of the various concentration of Alg-C coating on a solid substrates. Each point is the mean from 15 measurements on 3 replicate samples. The error bars display the 95% confidence limits.

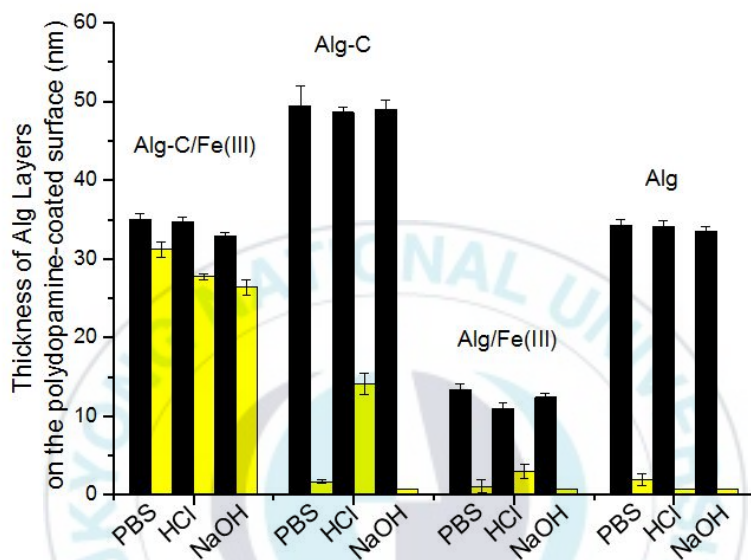


Figure 3.5 Thickness of Alg-C/Fe^{III}, Alg-C, Alg/Fe^{III}, and Alg layers on pDA-coated surfaces before (black) and after (yellow) chemical treatment. Each point is the mean from 15 measurements on 3 replicate samples. The error bars display the 95% confidence limits.

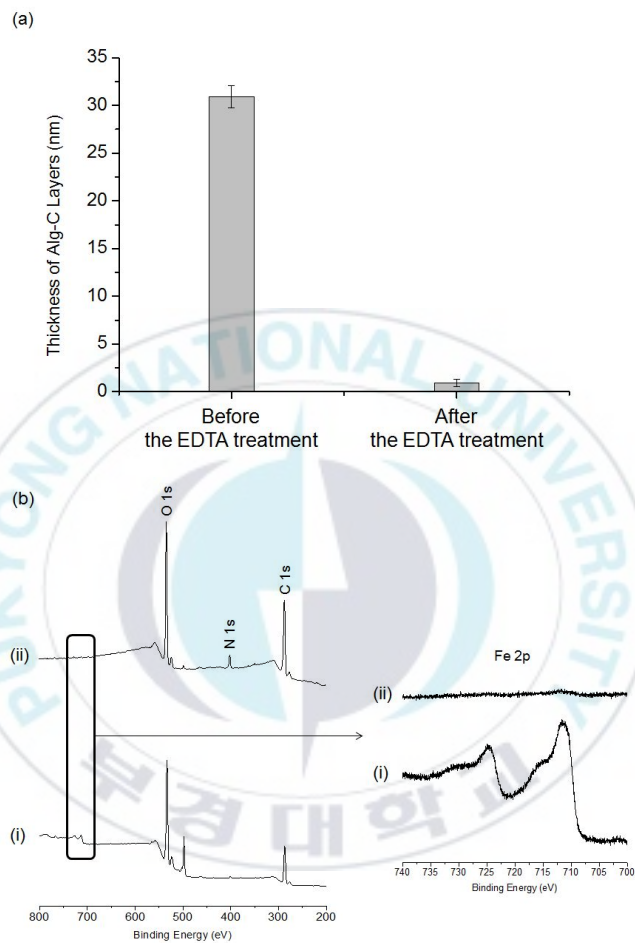


Figure 3.6 (a) Thickness of Alg-C layer on surfaces before (left) and after (right) EDTA treatment. Each point is the mean from 15 measurements on 3 replicate samples. The error bars display the 95% confidence limits. (b) XPS spectrum of the Alg-C layers on surfaces before (i) and after (ii) the EDTA treatment.

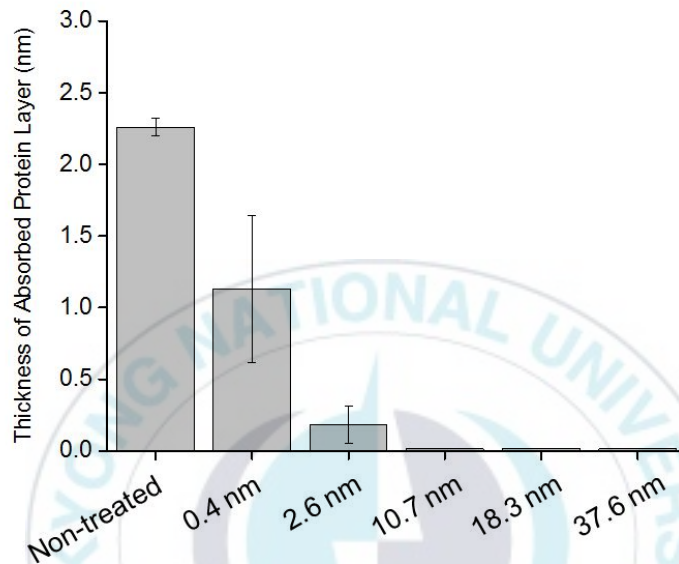


Figure 3.7 Protein adsorption on the various thickness of Alg-C layers. Each point is the mean from 15 measurements on 3 replicate samples. The error bars display the 95% confidence limits.

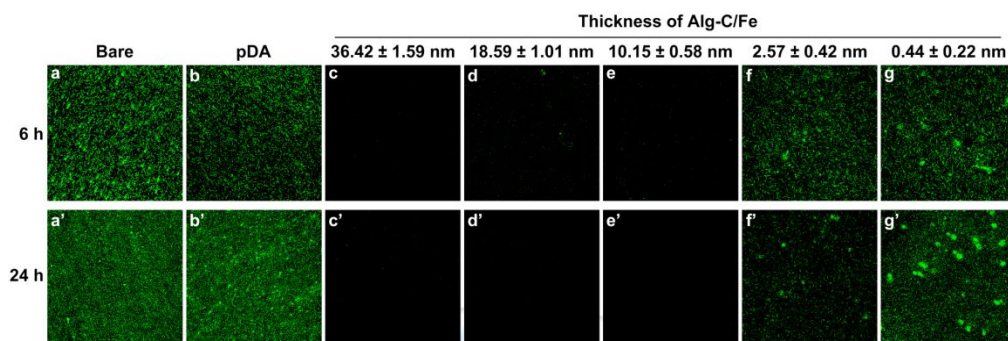


Figure 3.8 Antibacterial activity of Alg-C/Fe samples against *E. coli*. Representative fluorescence microscopic images of adherent *E. coli* cell to different substrates after incubation for 6 h (upper) or 24 h (lower).

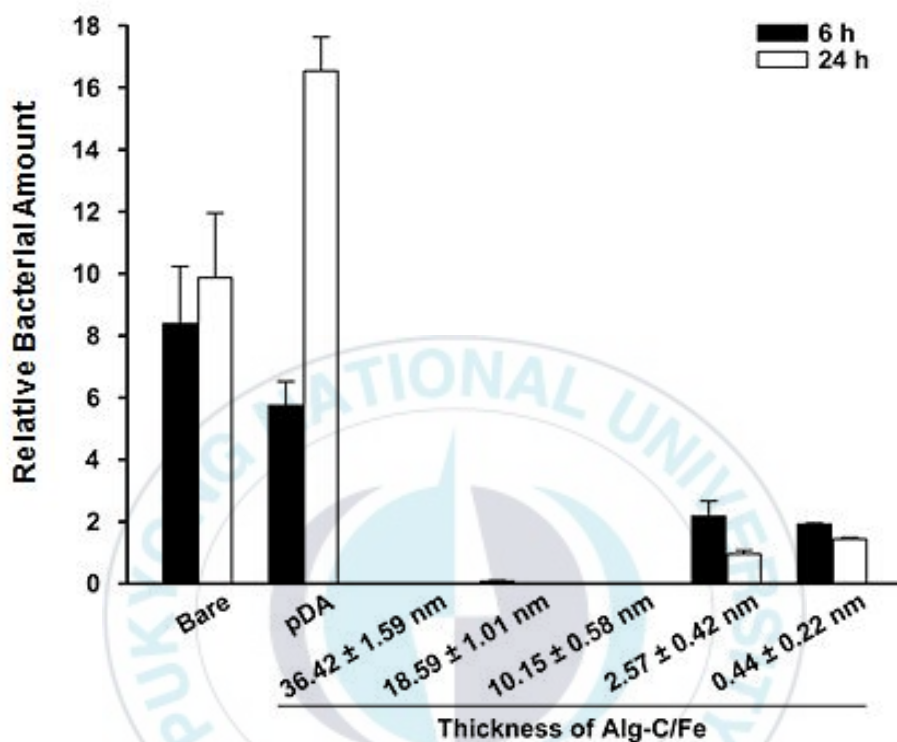


Figure 3.9 Density of *E. coli* cell adhered on the different substrates after incubation for (a) 6 h or (b) 24 h. Error bars represent the standard error of the mean (SEM) of three independent experiments.

3.4 Conclusions

We believe that our approach for constructing Alg-C layer on solid substrates could be one of simple and efficient antibacterial coatings as the coating method is very facile and rapid, assisted by spin-coating, and the coating thickness is able to be easily controlled by varying the concentration of Alg-C.

3.5 References

Banerjee, I.; Pangule, R. C.; Kane, R. S. **2011**. Antifouling Coatings: Recent Developments in the Design of Surfaces that Prevent Fouling by Proteins, Bacteria, and Marine organisms. *Adv. Mater.* *23*: 690-718.

Barrett, D. G.; Fullenkamp, D. E.; He, L.; Holten-Andersen, N.; Lee, K. Y. C.; Messersmith, P. B. **2013**. pH-Based Regulation of Hydrogel Mechanical Properties Through Mussel-Inspired Chemistry and Processing. *Adv. Funct. Mater.* *23*: 1111-1119.

Caro, A.; Humblot, V.; Méthivier, C.; Minier, M.; Salmain, M.; Pradier, C. M. **2009**. Grafting of Lysozyme and/or Poly(ethylene glycol) to Prevent Biofilm

Growth on Stainless Steel Surfaces. *J. Phys. Chem. B* 113: 2101-2109.

Castner, D. G.; Ratner, B. D. **2002**. Biomedical Surface Science: Foundations to Frontiers. *Surf. Sci.* 500: 28-60.

Cheng, G.; Zhang, Z.; Chen, S.; Bryers, J. D.; Jiang, S. **2007**. Inhibition of Bacterial Adhesion and Biofilm Formation on Zwitterionic Surfaces. *Biomaterials* 28: 4192-4199.

Cho, W. K.; Kong, B.; Choi, I. S. **2007**. Highly Efficient Non-Biofouling Coating of Zwitterionic Polymers: Poly((3-(methacryloylamino)propyl)-dimethyl(3-sulfopropyl) ammonium hydroxide). *Langmuir* 23: 5678-5682.

Faure, E.; Falentin-Daudre, C.; Lanero, T. S.; Vreuls, C.; Zocchi, G.; Van De Weerd, C.; Martial, J.; Jerome, Duwez, A. S.; Detrembleur, C. **2012**. Functional Nanogels as Platforms for Imparting Antibacterial, Antibiofilm, and Antiadhesion Activities to Stainless Steel. *Adv. Funct. Mater.* 22: 5271-5282.

Holten-Andersen, N.; Harrington, M. J.; Birkedal, H.; Lee, B. P.; Messersmith, P. B.; Lee, K. Y. C.; Waite, J. H. **2011**. PH-Induced Metal-Ligand Cross-Links Inspired by Mussel Yield Self-Healing Polymer Networks with Near-Covalent

Elastic Moduli. *Proc. Natl. Acad. Sci. U. S. A.* **108**: 2651-2655.

Karbassi, E.; Asadinezhad, A.; Lehocký, M.; Humpolíček, P.; Vesel, A.; Novák, I.; Sába, P. **2014**. Antibacterial Performance of Alginic Acid Coating on Polyethylene Film. *Int. J. Mol. Sci.* **15**: 14684-14696.

Kingshott, P.; Wei, J.; Bagge-Ravn, D.; Gadegaard, N.; Gram, L. **2003**. Covalent Attachment of Poly(ethylene glycol) to Surfaces, Critical for Reducing Bacterial Adhesion. *Langmuir* **19**: 6912-6921.

Lee, H.; Dellatore, S. M.; Miller, W. M.; Messersmith, P. B. **2007**. Mussel-Inspired Surface Chemistry for Multifunctional Coatings. *Science* **318**: 426-430.

Lee, H.; Lee, K. D.; Pyo, K. B.; Park, S. Y.; Lee, H. **2010**. Catechol-Grafted Poly(ethylene glycol) for PEGylation on Versatile Substrates. *Langmuir* **26**: 3790-3793.

Lee, K. Y.; Mooney, D. J. **2012**. Alginate: Properties and Biomedical Applications. *Prog. Polym. Sci.* **37**: 106-126.

Lee, Y. K.; Park, J. H.; Moon, H. T.; Lee, D. Y.; Yun, J. H.; Byun, Y. **2007**. The

Short-Term Effects on Restenosis and Thrombosis of Echinomycin-Eluting Stents Topcoated with a Hydrophobic Heparin-Containing Polymer. *Biomaterials* 28: 1523-1530.

Liu, Y.; Chang, C. P.; Sun, T. **2014**. Dopamine-Assisted Deposition of Dextran for Nonfouling Applications. *Langmuir* 30: 3118-3126.

Martwiset, S.; Koh, A. E.; Chen, W. **2006**. Nonfouling Characteristics of Dextran-Containing Surfaces. *Langmuir* 22: 8192-8196.

McArthur, S. L.; Mclean, K. M.; Kingshott, P.; St John, H. A. W.; Chatelier, R. C.; Griesser, H. J. **2000**. Effect of Polysaccharide Structure on Protein Adsorption. *Colloids Surf., B: Biointerface* 17: 37-48.

McLean, K. M.; Johnson, G.; Chatelier, R. C.; Beumer, G. J.; Steele, J. G.; Griesser, H. J. **2000**. Method of Immobilization of Carboxymethyl-Dextran Affects Resistance to Tissue and Cell Colonization. *Colloids Surf., B* 18: 221-234.

Morra, M.; Cassineli, C. **1999**. Non-Fouling Properties of Polysaccharide-Coated Surfaces. *J. Biomater. Sci. Polym. Ed.* 10: 1107-1124.

Morra, M.; Cassinelli, C. **1998**. Simple Model for the XPS Analysis of Polysaccharide-coated Surfaces. *Surf. Interface Anal.* 26: 742-746.

Morra, M.; Cassinelli, C. **1999**. Surface Studies on a Model Cell-Resistant System. *Langmuir* 15: 4658-4663.

Page, K.; Wilson, M.; Parkin, I. P. **2009**. Antimicrobial Surfaces and Their Potential in Reducing the Role of the Inanimate Environment in the Incidence of Hospital-Acquired Infections. *J. Mater. Chem.* 19: 3819-3831.

Park, J. Y.; Yeom, J.; Kim, J. S.; Lee, M.; Lee, H.; Nam, Y. S. **2013**. Cell-repellant Dextran Coatings of Porous Titania Using Mussel Adhesion Chemistry. *Macromol. Biosci.* 13: 1511-1519.

Unsworth, L. D.; Sheardown, H.; Brash, J. L. **2005**. Protein Resistance of Surfaces Prepared by Sorption of End-Thiolated Poly (ethylene glycol) to Gold: Effect of Surface Chain Density. *Langmuir* 21: 1036-1041.

Waite, J. H. **1999**. Reverse Engineering of Bioadhesion in Marine Mussels. *Ann. N. Y. Acad. Sci.* 875: 301-309.

Waite, J. H.; Qin, X. **2001**. Polyphosphoprotein from the Adhesive Pads of *Mytilus edulis*. *Biochemistry* 40: 2887-2893.

Waite, J. H.; Tanzer, M. L. **1981**. Polyphenolic Substance of *Mytilus edulis*: Novel Adhesive Containing L-Dopa and Hydroxyproline. *Science* 212: 1038-1040.

Wang, R.; Neoh, K. G.; Shi, Z.; Kang, E. T.; Tambyah, P. A.; Chiong, E. **2012**. Inhibition of *Escherichia coli* and *Proteus mirabilis* Adhesion and Biofilm Formation on Medical Grade Silicone Surface. *Biotechnol. Bioeng.* 109: 336-345.

Wei, Q.; Li, B.; Yi, N.; Su, B.; Yin, Z.; Zhang, F.; Li, J.; Zhao, C. **2011**. Improving the Blood Compatibility of Material Surfaces via Biomolecule-Immobilized Mussel-Inspired Coatings. *J. Biomed. Mater. Res., Part A* 96: 38-45.

Wen, Y.; Oh, J. K. **2014**. Recent Strategies to Develop Polysaccharide-Based Nanomaterials for Biomedical Applications. *Macromol. Rapid Commun.* 35: 1819-1832.

Yoshioka, T.; Tsuru, K.; Hayakawa, S.; Osaka, A. **2003**. Preparation of Alginic Acid Layers on Stainless-Steel Substrates for Biomedical Applications.

Biomaterials 24: 2889-2894.

You, I.; Kang, S. M.; Byun, Y.; Lee, H. **2011**. Enhancement of Blood Compatibility of Poly(urethane) Substrates by Mussel-Inspired Adhesive Heparin Coating. *Bioconjugate Chem.* 22: 1264-1269.

Yu, Jing.; Wei, W.; Danner, E.; Ashley, R. K.; Israelachvili, J. N.; Waite, J. H. **2011**. Mussel Protein Adhesion Depends on Interprotein Thiol-Mediated Redox Modulation. *Nat. Chem. Biol.* 7: 588-590.

Zeng, H.; Hwang, D. S.; Israelachvili, J. N.; Waite, J. H. **2010**. Strong Reversible Fe³⁺-Mediated Bridging between Dopa-Containing Protein Films in Water. *Proc. Natl. Acad. Sci. U. S. A.* 107: 12850-12853.

Zhu, L. P.; Jiang, J. H.; Zhu, B. K.; Xu, Y. Y. **2011**. Immobilization of Bovine Serum Albumin onto Porous Polyethylene Membranes Using Strongly Attached Polydopamine as a Spcer. *Colloids Surf., B* 86: 111-118.

Abstract (Korean)

해양생물을 모방한 기능성 소재 및 표면 개발 연구

김 수 업

부경대학교 대학원 수산생물학과

최근 생물부착방지 표면에 대한 연구가 크게 관심 받고 있는데, 이는 의료장비, 바이오센서, 그리고 해양장비 분야에 응용되고 있다. 부착 방지성 표면을 제작하기 위해서 다양한 분자재료가 표면에 도입되어 왔으며, 대표적인 예로 다당류(polysaccharide), 폴리에틸렌글리콜 (polyethylene glycol), 그리고 양쪽성 이온 고분자 (zwitterionic polymer) 가 사용되어 왔다. 비록 앞서 언급된 재료들은 표면에 고정되어 표면에서의 우수한 생물 부착방지 기능을 보여주었으나, 복잡한 화학반응이 수반되고 소재 제한적이라는 결점을 가지고 있다. 이번 연구에서는 이러한 문제점을 해결하기 위하여 홍합을 모방한 기능성 고분자인 폴리도파민 (polydopamine) 을 표면에 도입하였다. 왜냐하면 폴리도파민 표면코팅 방법은 간편하며 표면 소재 종류에 관계없이 다양한 표면에 도입 가능한 장점을 가지기 때문이다. 최종적으로 홍합을 모방한 폴리도파민과 생물 부착방지 기능을 가진 분자재료를 결합하여 다양한 표면에 부착 방지 특성을 부여하는 것이 본 실험의 주목적이다. 첫 번째로, 홍합 족사 큐티클 특성을 모방하여 가역적 특성의 layer-by-layer (LbL) 증착 기법을 통해 표면을 계면 하였다. LbL 필름의 형성 방법은 폴리도파민이 코팅된 표면에 3 가 철 이온이 포함된 용액과 카테콜 화합물을 포함하고 있는 타닌산(TA) 용액을 순차적 담금 처리 하였다. 두 번째로, 간편하고 다양한 표면소재에 접목 가능한 해양생물 부착방지 표면 코팅 방법에 대해서 연구를 진행하였다. 해양생물 부착방지 표면 개발은 폴리도파민과 타닌산이 결합된 표면에 폴리에틸렌글리콜을 고정화 하였다. 폴리도파민이 코팅된 표면에 3 가 철 처리를 이용한 배위결합을 통하여 타닌산을 코팅 하였고, 폴리에틸렌글리콜의 고정은 수소결합을 통해 타닌산이 코팅된 표면에 도입 하였다. 이를 이용하여 스테인리스 스틸과 나일론 표면을 성공적으로 계면 하였고, 폴리에틸렌글리콜이 고정된 표면은 해양 규조류의 부착을 상당히 저해시킬 수 있었다. 마지막으로, 홍합의 접착 작용기인 카테콜 (catechol)이 도입 된 알긴산 (alginate)을 이용하여 박테리아 부착방지 나노필름을 제작 하였다. 알긴산-카테콜 나노필름은 폴리도파민이 코팅된 표면에 3 가 철의 배위결합을 통해 형성 하였고, 계면 된 표면은 대장균의 부착을 높은 효율로 방지할 수 있었다.